Regional Inflation Spillovers and Monetary Policy Design: Evidence from Peru's Successful Inflation-Targeting Framework

Aguilar, José and Quineche, Ricardo

Central Reserve Bank of Peru, Universidad del Pacífico (Lima, Perú), Pontificia Universidad Católica del Perú (Lima, Perú)

23 July 2025

REGIONAL INFLATION SPILLOVERS AND MONETARY POLICY DESIGN: EVIDENCE FROM PERU'S SUCCESSFUL INFLATION-TARGETING FRAMEWORK*

A PREPRINT

José Aguilar
Central Bank of Peru
Pontificia Universidad Católica del Perú (Lima, Perú)
j.aguilar@pucp.edu.pe

Ricardo Quineche
Universidad del Pacífico (Lima, Perú)
Central Bank of Peru
r.quinecheu@up.edu.pe

July 25, 2025

ABSTRACT

Despite being an emerging economy, Peru has achieved superior post-pandemic disinflation compared to major developed economies, making its regional inflation dynamics globally instructive for monetary policy design. This study investigates Lima's suitability as Peru's inflation-targeting anchor by analyzing regional spillovers across nine economic regions using monthly CPI data (2002-2024). Employing both Diebold-Yilmaz time-domain and Baruník-Křehlík frequency-domain frameworks, we quantify the direction, magnitude, and persistence of inflation transmission. Results reveal strong regional interdependence (73.60% total spillover index) with Lima as the dominant net transmitter (23.94 percentage points). However, frequency decomposition uncovers striking cyclical heterogeneity: Lima receives short-run shocks from food-producing regions but dominates long-run transmission (44.70% vs. 28.99% frequency spillover index). Rolling-window analysis during COVID-19 shows temporary spillover disruption (connectivity declining from 75% to 68%) followed by recovery during 2022's inflationary surge. Robustness checks across specifications, granular city-level data, and three-band frequency segmentation confirm Lima's structural centrality at lower frequencies. These findings validate the Central Reserve Bank's Lima-centered approach for long-run targeting while revealing asymmetric frequency-dependent spillovers. The presence of short-run regional shocks suggests integrating upstream agricultural signals could enhance near-term forecasting and policy responsiveness.

Keywords Inflation spillovers · Regional inflation dynamics · Frequency-domain analysis · Diebold-Yilmaz methodology · Baruník-Křehlík framework

*The views expressed in this document are solely those of the authors and do not necessarily reflect the position of the Central Reserve Bank of Peru.

1 Introduction

In the architecture of modern monetary policy, few central banks face as complex a challenge as maintaining price stability across economically diverse regions while operating under constraints imposed by geographical heterogeneity and structural asymmetries. Peru's Central Reserve Bank (BCRP) exemplifies this challenge, having achieved remarkable success in inflation targeting despite governing an economy characterized by pronounced regional disparities, partial financial dollarization, and center-periphery dynamics that fundamentally shape how monetary policy transmits across space and time.

Since adopting full-fledged inflation targeting in 2002, the BCRP has garnered international recognition for its monetary policy credibility and institutional excellence. Governor Julio Velarde has received prestigious accolades including Central Banker of the Year from The Banker (2015, 2020, 2022), Best Central Banker from Global Finance (2015, 2016), and Central Bank Governor of the Year from LatinFinance (2016). These honors reflect not merely institutional recognition but empirical success: Peru has achieved the lowest average inflation (2.6 percent annually since 2001) and highest growth rate (5.8 percent between 2005-2014) among the five largest Latin American inflation-targeting countries, despite facing similar external shocks and structural challenges. Most remarkably, Peru's post-pandemic disinflation has outperformed major developed economies—successfully reducing inflation from 8.66% in January 2023 to precisely 2.0% by December 2024, achieving the center of its target range while the United States struggled with 2.9% inflation, Japan reached 3.6%, the eurozone averaged 2.4%, and the OECD collectively remained at 4.5%. This exceptional performance demonstrates that Peru, an emerging economy, has achieved superior monetary policy transmission and expectation anchoring compared to advanced economies with decades more experience in inflation targeting—making the analysis of Peru's regional inflation dynamics not merely academically interesting, but globally instructive for monetary policy design.

However, this policy success rests on a foundational choice that distinguishes Peru from most modern central banks: the BCRP anchors its inflation-targeting framework to Lima's Consumer Price Index rather than a nationally aggregated measure. This operational decision-uncommon among contemporary central banks-raises fundamental questions about regional representativeness, spatial equity in monetary policy transmission, and the empirical justification for center-based inflation targeting in economically heterogeneous countries.

The study of inflation spillovers has evolved significantly over the past two decades, moving from static correlation-based approaches to dynamic, directional, and frequency-sensitive frameworks. A major methodological leap came with Diebold and Yilmaz (2009, 2012), who introduced a spillover index based on forecast error variance decompositions from vector autoregressions. Building on this foundation, Baruník and Křehlík (2018) extended the approach into the frequency domain, enabling decomposition of spillovers across different time horizons-particularly relevant for inflation analysis, as it distinguishes between short-term volatility and long-term persistence.

Empirical applications of these methods to inflation spillover analysis have expanded rapidly, yet they remain heavily skewed toward advanced economies (Elsayed et al., 2021; Jordan, 2016; Pham and Sala, 2022; Tiwari et al., 2019; Wen et al., 2021).[2] This geographic bias represents a significant gap, given that emerging economies often face more complex spillover dynamics due to greater exposure to external shocks and more pronounced regional heterogeneity.

At the subnational level, research remains remarkably limited despite its obvious policy relevance. Çakır (2023) uses the Diebold-Yilmaz framework on Turkey's regional data, while Istiak et al. (2021) pioneer the frequency-domain approach for the G7. Despite Peru's prominence in inflation-targeting success stories, regional inflation spillovers within the country remain underexplored. Winkelried and Gutierrez (2015) emphasize Lima's central role in shaping national inflation trends, but their analysis does not employ modern spillover methodologies or assess the frequency-dependent nature of regional transmission.

This study addresses the critical gap by applying complementary spillover methodologies to monthly CPI data from 2002 to 2024 across Peru's nine economic regions. We employ both the time-domain Diebold-Yilmaz (DY) approach and the frequency-domain Baruník-Křehlík (BK) framework to investigate: (1) the direction and magnitude of inflation spillovers across regions; (2) how spillover patterns vary across cyclical frequencies; and (3) how spillover dynamics have evolved over time, particularly during crisis periods.

Our comprehensive analysis yields several striking findings. The time-domain analysis reveals substantial regional interdependence (73.60% total spillover index) with Lima as the dominant net transmitter (23.94 percentage points). However, the frequency decomposition uncovers a more nuanced picture: Lima functions as a net recipient of short-run shocks from food-producing regions but dominates as a transmitter over longer horizons (44.70% vs. 28.99% frequency

[2]These connectedness methodologies have also seen wide application across diverse fields: commodity-market integration (Lucey et al., 2014; Batten et al., 2015); global business-cycle dynamics (Diebold and Yilmaz, 2015); oil-price and policy-uncertainty spillovers (Antonakakis et al., 2014).

spillover index). Rolling-window analysis during COVID-19 shows temporary spillover disruption followed by recovery during 2022's inflationary surge, demonstrating both vulnerability and resilience of transmission mechanisms.

These findings provide strong empirical validation for the BCRP's continued use of Lima's CPI as the primary inflation-targeting anchor, given Lima's structural dominance in long-run spillovers-as reflected in its role in anchoring inflation expectations (Quineche et al., 2024). However, the frequency-domain results suggest concrete improvements to forecasting methodology by integrating upstream agricultural signals from food-producing regions, which could enhance near-term projection accuracy. The COVID-19 analysis suggests the need for adaptive policy responses during crisis periods when normal transmission channels may be disrupted.

While focused on Peru, this research addresses broader questions relevant to emerging economies worldwide. The methodology provides a general framework for analyzing regional inflation dynamics in spatially diverse economies. Countries like Brazil, India, South Africa, and Mexico face similar challenges in designing monetary policy for economically heterogeneous regions (Ndou and Gumata, 2017; de Guzmán and Salas, 2023; Bhoi et al., 2020; Colunga-Ramos and Cepeda, 2023). The findings also contribute to theoretical understanding of monetary policy transmission, suggesting that optimal policy design should account for both short-run supply-side shocks from peripheral regions and long-run demand-side transmission from economic centers.

This research provides the first comprehensive analysis of regional inflation spillovers in Peru using modern spillover methodologies, validates the empirical foundation of the BCRP's Lima-centered inflation targeting framework, and offers a generalizable approach for analyzing subnational monetary transmission in emerging economies globally.

The remainder of this paper unfolds as follows. Section 2 introduces the regional inflation dataset and aggregation methodology. Section 3 presents the empirical methodology, explaining both the time-domain and frequency-domain spillover frameworks. Section 4 reports and interprets the empirical findings, including static spillover patterns, dynamic evolution, and robustness checks. Section 5 concludes with detailed policy implications for the BCRP and broader lessons for regional inflation management in emerging economies.

2 Regional Inflations

This study employs monthly Consumer Price Index (CPI) data with base December 2021=100 for Peru's 25 largest cities, published by the National Institute of Statistics and Informatics (INEI), spanning January 2002 to December 2024. To ensure temporal consistency, we retroactively extended the December 2021 base backward by applying monthly percentage changes from the previous 2009-based index, creating a unified 23-year time series that captures both structural changes and cyclical variations in regional price dynamics.

Following the established framework of Winkelried and Gutierrez (2015), we adopt the economic classification of Peruvian cities into nine economic regions proposed by Gonzales de Olarte (2003). This classification, summarized in Table 1, is grounded in both historical considerations-as regions comprise contiguous departments with shared cultural and administrative legacies-and economic factors, including market articulation, trade integration, and production specialization. The nine-region framework effectively captures Peru's economic geography, from Lima's urban concentration to the Amazon's resource extraction, the coast's agricultural production, and the highlands' mining activities.

To construct regional price indices, we employ a weighted additive approach where each city's CPI is weighted according to its respective share in national consumption patterns.[3] The aggregated regional CPI is calculated as:

$$\mathrm{CPI}_{r,t} = \frac{\sum_{i \in r} w_i \cdot \mathrm{CPI}_{i,t}}{\sum_{i \in r} w_i}, \tag{1}$$

where $\mathrm{CPI}_{r,t}$ denotes the Consumer Price Index for region r at time t, w_i is the weight of department i within region r, and $\mathrm{CPI}_{i,t}$ is the Consumer Price Index of department i at time t. This weighting scheme ensures that regional inflation measures accurately reflect the relative economic importance of each city within its region while maintaining consistency with national inflation calculations.

Based on the regional Consumer Price Indices, monthly inflation for region r at time t is computed as:

$$\mathbf{x}_{r,t} = 100 \times \left(\log \mathrm{CPI}_{r,t} - \log \mathrm{CPI}_{r,t-1}\right). \tag{2}$$

[3]Although INEI updated the CPI base to December 2021=100 and now publishes indices using this new base, the revised expenditure weights by department are not publicly available. As a result, regional aggregation continues to rely on the weights from the 2009 base.

Table 1: Economic regions in Perú

Region	Cities (weights)
1	Lima (66.02)
2	Piura (2.01), Tumbes (0.56)
3	Chiclayo (2.55), Cajamarca (1.14), Chachapoyas (0.14)
4	Trujillo (4.60), Chimbote (2.05), Huaraz (0.58)
5	Ica (1.31), Ayacucho (0.70), Huancavelica (0.19)
6	Arequipa (4.94), Moquegua (0.30), Tacna (1.55), Puno (0.76)
7	Huánuco (0.81), Cerro de Pasco (0.34), Huancayo (1.91)
8	Abancay (0.34), Cusco (2.72), Puerto Maldonado (0.48)
9	Iquitos (1.99), Moyobamba (0.64), Pucallpa (1.30)

Notes: Classification of Peruvian Departments into 9 economic regions, following Gonzales de Olarte (2003, p. 41). Numbers in parentheses indicate the weights used for national inflation calculations by INEI.The weights reflect the national expenditure shares utilized in computing inflation using the 2009 base year.

This log-difference specification provides several analytical advantages: it yields approximately percentage changes for small variations, ensures stationarity properties essential for spillover analysis, and facilitates direct comparison across regions with different price levels.

Figure 1 illustrates monthly inflation across Peru's nine economic regions, revealing both striking synchronization and notable heterogeneity in regional price dynamics. Despite considerable differences in volatility and amplitude across regions, the time series exhibit a remarkably synchronized pattern, indicating the influence of shared macroeconomic and structural factors on regional price formation. This co-movement provides preliminary evidence of substantial spillover effects that our formal analysis will quantify.

Three major inflationary episodes, highlighted in Figure 1, demonstrate how external shocks propagate through Peru's regional system:

- The 2007-2009 Global Commodity Boom: The first major episode coincided with the global commodity price surge, which drove up food and energy costs worldwide. In Peru, this translated to synchronized inflation increases across all regions, with food-producing areas (Regions 3 and 7) experiencing particularly pronounced spikes that subsequently transmitted to other regions. This episode illustrates how global supply shocks can amplify regional disparities before eventually synchronizing national inflation dynamics (Moreno, 2009).
- The 2017 *Coastal El Niño* Event: The sharp but short-lived spike in March 2017 aligns with the Coastal El Niño phenomenon, which severely disrupted transportation and logistics networks in northern and central Peru. This event provides a natural experiment in regional shock transmission: the initially localized supply disruptions in coastal regions rapidly propagated inland through supply chain linkages, leading to temporary but significant price pressures across the national economy (Yglesias-González et al., 2023). The rapid diffusion and subsequent normalization demonstrate both the vulnerability and resilience of Peru's regional price system.
- The 2021-2023 Pandemic and Geopolitical Inflation: The most recent episode reflects the complex interaction of pandemic-related supply chain disruptions and elevated international food and energy costs stemming from the Russia-Ukraine conflict. Unlike previous episodes that originated domestically or affected specific sectors, this global shock simultaneously impacted all regions through multiple transmission channels: supply chain fragmentation, energy price pass-through, and exchange rate depreciation (Banco Central de Reserva del Perú, 2023). The synchronized response across regions, despite varying degrees of international integration, underscores the increasing interconnectedness of Peru's regional economies.

The observed temporal co-movement of regional inflation—particularly pronounced during major inflationary episodes—provides compelling preliminary evidence of meaningful domestic spillovers. Simple correlation analysis, shown in Table 2, reveals that all regional inflation series are positively correlated, with an average correlation of 0.59 across all regional pairs. These correlations, while substantial, vary meaningfully across region pairs, suggesting that spillover effects are neither uniform nor complete, motivating the need for directional spillover analysis.

Summary statistics reported in Table 3 reveal important heterogeneity in regional inflation characteristics. Lima (Region 1) exhibits the lowest level of inflation volatility (standard deviation of 0.33), despite its central role, consistent with its

Table 2: Correlation matrix

	Lima	Region 2	Region 3	Region 4	Region 5	Region 6	Region 7	Region 8	Region 9
Lima	1.000								
Region 2	0.699***	1.000							
Region 3	0.750***	0.764***	1.000						
Region 4	0.754***	0.777***	0.762***	1.000					
Region 5	0.734***	0.613***	0.673***	0.709***	1.000				
Region 6	0.578***	0.535***	0.554***	0.579***	0.596***	1.000			
Region 7	0.713***	0.605***	0.690***	0.709***	0.713***	0.602***	1.000		
Region 8	0.376***	0.319***	0.411***	0.425***	0.499***	0.662***	0.569***	1.000	
Region 9	0.584***	0.595***	0.618***	0.579***	0.612***	0.441***	0.559***	0.369***	1.000

Note: This table reports the correlation coefficients of regional inflation rates along with their statistical significance: *** denotes significance at the 1% level, ** at the 5% level, and * at the 10% level.

diversified economic base and sophisticated distribution networks. In contrast, regions such as Region 2 (0.52), Region 4 (0.48), and Region 8 (0.48) show higher volatility, likely reflecting greater exposure to agricultural supply disruptions, seasonal demand fluctuations, and localized logistical constraints. In terms of distributional shape, Lima also displays the lowest excess kurtosis (0.80), suggesting relatively stable inflation dynamics. By comparison, most other regions exhibit more pronounced kurtosis, especially Regions 2 and 3 (2.78 and 2.30, respectively), both agricultural producers. These values indicate a higher frequency of extreme inflation realizations, consistent with the presence of price spikes in food-related sectors.

The presence of occasional extreme values-particularly in agricultural and resource-dependent regions-motivates our choice of spillover methodologies that can accommodate non-normal distributions and capture directional transmission effects. The combination of strong co-movement with persistent regional heterogeneity suggests a complex spillover structure where some regions consistently transmit shocks while others primarily receive them-precisely the type of asymmetric relationship that modern spillover indices are designed to quantify.

Finally, Table 3 also presents the results of the Augmented Dickey–Fuller (ADF) and Phillips–Perron (PP) unit root tests applied to the monthly regional inflation series. In all cases, the null hypothesis of nonstationarity is rejected. These results justify the use of a generalized VAR framework to compute spillover indices following DY and BK approaches.

Table 3: Summary statistics

	Lima	Region 2	Region 3	Region 4	Region 5	Region 6	Region 7	Region 8	Region 9
Mean	0.254	0.296	0.280	0.282	0.318	0.298	0.286	0.296	0.254
Std. Dev.	0.331	0.521	0.436	0.484	0.383	0.449	0.338	0.478	0.414
Skewness	0.580	0.808	0.538	0.304	0.358	-0.047	0.739	0.434	0.705
Kurtosis	0.800	2.781	2.299	1.531	1.559	3.627	1.110	2.085	2.486
ADF	-3.655***	-3.368**	-3.590***	-3.999***	-3.416**	-4.209***	-2.978**	-3.564***	-3.456**
PP	-13.017***	-12.493***	-12.005***	-13.647***	-12.638***	-10.062***	-11.041***	-10.643***	-11.621***

Notes: The table reports the test statistics from the Augmented Dickey-Fuller (ADF) and Phillips-Perron (PP) unit root tests. For the ADF test, the lag length was selected based on the t-statistic criterion. *** denotes significance at the 1% level, ** at the 5% level, and * at the 10% level.

To quantify these interregional linkages formally and identify the directional transmission of inflationary shocks, we apply spillover indices derived from forecast-error variance decompositions. The analytical framework for this analysis is presented in Section 3, followed by comprehensive empirical results in Section 4 .

Figure 1: Monthly regional inflations

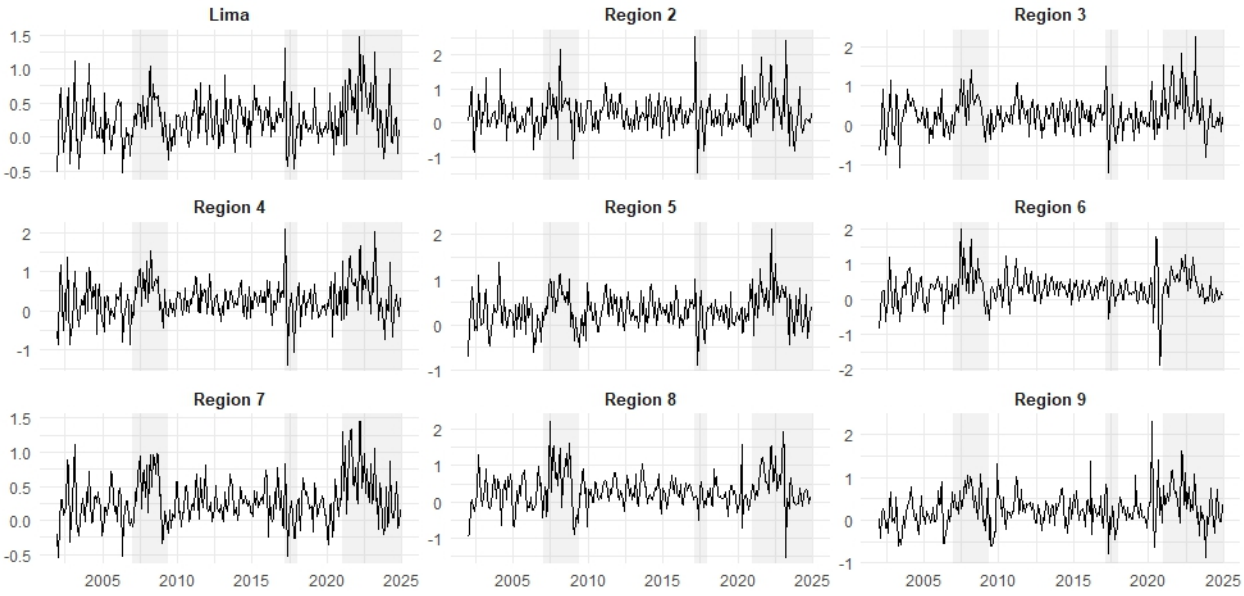

3 Empirical Methodology

3.1 Time-Domain Spillover Estimation: Diebold-Yilmaz Approach

To quantify inflation spillovers among Peru's economic regions, this study applies the time-domain framework introduced by Diebold and Yilmaz (2012), which enables dynamic connectedness estimation among multiple time series through generalized forecast error variance decomposition (GFEVD) of a vector autoregressive (VAR) model.

Let $\mathbf{x}_t = (x_{1t}, x_{2t}, \ldots, x_{nt})'$ be an n-dimensional vector of monthly inflation rates across the nine economic regions, modeled as a VAR(p) process:

$$\Phi(L)\mathbf{x}_t = \boldsymbol{\varepsilon}_t, \tag{3}$$

where $\Phi(L)$ is a matrix lag polynomial of order p, and $\boldsymbol{\varepsilon}_t$ is a vector of serially uncorrelated shocks. Assuming stationarity, this can be rewritten in moving average form:

$$\mathbf{x}_t = \Psi(L)\boldsymbol{\varepsilon}_t, \tag{4}$$

where $\Psi(L)$ captures the dynamic responses of the system to shocks over time. Connectedness is estimated using GFEVD, which computes the proportion of forecast error variance of region j attributable to shocks in region k over horizon H:

$$\theta_{jk}^{(H)} = \text{GFEVD contribution from region } k \text{ to region } j. \tag{5}$$

Because shocks are not orthogonalized, rows may not sum to unity; thus, we normalize each element as:

$$\tilde{\theta}_{jk}^{(H)} = \frac{\theta_{jk}^{(H)}}{\sum_{k=1}^{n} \theta_{jk}^{(H)}}. \tag{6}$$

The Total Spillover Index (TSI) is defined as:

$$\text{TSI}^{(H)} = 100 \times \frac{\sum_{j \neq k} \tilde{\theta}_{jk}^{(H)}}{\sum_{j,k} \tilde{\theta}_{jk}^{(H)}}, \tag{7}$$

representing the percentage of system-wide forecast variance attributable to cross-regional shocks. Directional spillovers are computed to identify net transmitters and receivers:

$$\text{Spillovers TO region } j = \sum_{k \neq j} \tilde{\theta}_{jk}^{(H)}, \tag{8}$$

$$\text{Spillovers FROM region } j = \sum_{k \neq j} \tilde{\theta}_{kj}^{(H)}, \tag{9}$$

$$\text{NET Spillover for region } j = \text{FROM} - \text{TO}. \tag{10}$$

We also compute the NET pairwise spillovers to captures the directional influence that region j exerts on region k (and vice versa) in net terms. This measure is computed as:

$$\text{NET pairwise spillover between j and k} = \frac{\tilde{\theta}_{jk}^{(H)} - \tilde{\theta}_{kj}^{(H)}}{n} \tag{11}$$

To capture time variation in spillover intensity, the GFEVD is computed using a rolling window of fixed length (e.g., 150 months), enabling analysis of evolving patterns over Peru's inflation dynamics between 2002 and 2024.

This framework allows a rigorous evaluation of Lima's role as a transmitter or receiver of inflationary shocks, providing empirical insight into its suitability as the Central Reserve Bank of Peru's operational benchmark.

3.2 Frequency-Domain Spillover Estimation: Baruník-Krehlík Approach

To complement the time-domain analysis, this study adopts the frequency-domain connectedness framework proposed by Baruník and Křehlík (2018), which allows for the decomposition of inflation spillovers across different frequency bands. This method distinguishes between short-term fluctuations and long-run persistence in spillover dynamics—an essential feature for analyzing the transmission of inflation from Lima to other Peruvian regions.

Let $\mathbf{x}_t$ denote the n-dimensional vector of monthly inflation rates across Peru's nine economic regions. Assuming a stationary VAR representation, the process admits a moving average form:

$$\mathbf{x}_t = \sum_{h=0}^{\infty} \mathbf{\Psi}_h \boldsymbol{\varepsilon}_{t-h}, \tag{12}$$

where $\mathbf{\Psi}_h$ are impulse response matrices and $\boldsymbol{\varepsilon}_t$ is a vector of serially uncorrelated shocks. Applying the Fourier transform yields the frequency response function:

$$\mathbf{\Psi}(e^{-i\omega}) = \sum_{h=0}^{\infty} \mathbf{\Psi}_h e^{-i\omega h}, \tag{13}$$

which captures how inflation shocks transmit across frequencies $\omega \in (-\pi, \pi)$.

The generalized causation spectrum, which quantifies the share of variance in region j due to shocks in region k at frequency ω, is computed as:

$$f_{jk}(\omega) = \frac{\left| \left(\mathbf{\Psi}(e^{-i\omega}) \mathbf{\Sigma} \mathbf{\Psi}^*(e^{i\omega}) \right)_{jk} \right|^2}{\left(\mathbf{\Psi}(e^{-i\omega}) \mathbf{\Sigma} \mathbf{\Psi}^*(e^{i\omega}) \right)_{jj}}, \tag{14}$$

where $\mathbf{\Sigma}$ is the covariance matrix of innovations and $*$ denotes the complex conjugate transpose.

The spillover within a given frequency band $d = (\omega_a, \omega_b)$ is calculated by integrating the causation spectrum, weighted by the power of region j at that frequency:

$$\theta_{jk}^{(d)} = \frac{1}{2\pi} \int_{\omega_a}^{\omega_b} \gamma_j(\omega) f_{jk}(\omega)\, d\omega, \tag{15}$$

where $\gamma_j(\omega)$ is the spectral density of region j. Normalization yields the relative contribution:

$$\tilde{\theta}_{jk}^{(d)} = \frac{\theta_{jk}^{(d)}}{\sum_{k=1}^{n} \theta_{jk}^{(d)}}. \tag{16}$$

The frequency-specific spillover index (FSI) is given by:

$$\text{FSI}^{(d)} = 100 \times \frac{\sum_{j \neq k} \tilde{\theta}_{jk}^{(d)}}{\sum_{j,k} \tilde{\theta}_{jk}^{(d)}}, \tag{17}$$

capturing the share of cross-regional inflation variance on the band d. Similar to the time-domain approach, directional spillovers are also constructed on the frequency band d.

For this study, we divide the spectrum into two bands:$(\pi, \pi/3)$, which captures short-term movements; and $(\pi/3, 0)$, which reflects longer-term interactions. Rolling-window estimation is used to trace spillover dynamics over time, revealing Lima's changing role as an inflation transmitter or receiver. This dual-frequency approach provides deeper insight into Lima's influence on both immediate and persistent regional inflation movements—informing the assessment of its validity as the Central Reserve Bank's operational benchmark.

4 Empirical Results

4.1 Time domain spillovers

To explore the interconnectedness of regional inflation dynamics across Peru's economic landscape, we begin by applying the time-domain spillover framework introduced by Diebold and Yilmaz (2012). This methodology is implemented in both static and dynamic forms: the static version provides a comprehensive full-sample overview of inflation spillover patterns and regional hierarchies, while the dynamic specification employs a rolling-window approach to trace the temporal evolution of regional connectedness through major economic episodes and structural changes.

4.1.1 Static Inflation Spillovers Architecture

We commence our empirical analysis by examining the static properties of inflation spillovers across Peru's nine economic regions using a vector autoregressive (VAR) model with one lag and a three-month forecast horizon. The lag specification is selected using the Bayesian Information Criterion (BIC) to balance model parsimony with adequate dynamic representation, while the three-month horizon captures medium-term spillover effects relevant for monetary policy decision-making.

Table 4 presents the comprehensive inflation spillover matrix, where each element quantifies the proportion of forecast error variance of inflation in region i (row) attributable to shocks originating in region j(column). Diagonal entries capture own-region contributions to forecast variance, representing the degree of regional inflation autonomy, while off-diagonal values measure cross-regional spillovers that constitute the core of our analysis. The FROM column reports the total share of forecast error variance in each region explained by shocks from all other regions, effectively measuring each region's exposure to external influences. Conversely, the TO row reflects the total spillovers transmitted by each region to the rest of the system, quantifying each region's systemic influence. The NET measure-defined as the difference between TO and FROM-provides the crucial indicator of whether a region is a net transmitter (positive values) or net recipient (negative values) of inflationary shocks. Finally, the Total Spillover Index (TSI) summarizes the overall share of forecast error variance attributable to cross-regional spillovers, serving as a global measure of inflation interdependence.

To assess statistical significance, we implement a bootstrap procedure with 5,000 replications following Patton (2013) and Fousekis and Tzaferi (2021). Wald-type test statistics are computed under the null hypothesis of zero spillovers, with the test statistic defined as $\Theta = (R\hat{\Phi})'(RV_{\hat{\Phi}}R')^{-1}(R\hat{\Phi})$, where R denotes the restriction matrix, $\hat{\Phi}$ is the vector

Table 4: Time domain spillovers

	Lima	Region 2	Region 3	Region 4	Region 5	Region 6	Region 7	Region 8	Region 9	FROM
Lima	23.51	10.43	11.89	12.35	12.46	8.14	11.71	2.87	6.65	76.49***
Region 2	12.69	24.04	13.47	13.46	8.78	8.27	9.24	2.67	7.38	75.96***
Region 3	14.13	13.12	21.82	12.31	9.52	7.68	10.24	4.09	7.07	78.18***
Region 4	14.77	13.10	12.26	21.52	10.42	7.73	11.21	3.14	5.84	78.48***
Region 5	15.05	8.49	9.13	10.95	23.87	8.67	11.43	5.23	7.18	76.13***
Region 6	10.37	8.61	7.46	8.70	9.47	31.63	9.40	11.06	3.30	68.37***
Region 7	14.05	8.58	10.64	10.98	11.25	8.19	24.50	5.83	5.97	75.50***
Region 8	7.64	4.10	5.32	6.18	8.12	15.12	12.30	38.07	3.15	61.93***
Region 9	11.74	9.64	8.62	8.91	10.94	8.31	8.84	4.41	28.59	71.41***
TO	100.43***	76.06***	78.80***	83.84***	80.97***	72.13***	84.37***	39.30***	46.54***	
NET	23.94***	0.10	0.62	5.36	4.84	3.76	8.87***	-22.62***	-24.87***	TSI = 73.60***

Note: This table reports the static time domain spillovers across regions of Peru. For the TSI, TO, FROM and NET spillover measures, we report statistical significance: *** significant at the 1% level, ** at the 5% level, and * at the 10% level.

of point estimates, and $V_{\hat{\Phi}}$ is the bootstrap variance-covariance matrix. This rigorous statistical framework enables formal inference for the TSI, FROM, TO, and NET measures, providing confidence in our spillover estimates.

The TSI, estimated at 73.60% and statistically significant at the 1% level, reveals that nearly three-quarters of inflation forecast error variance across Peru's regions can be attributed to cross-regional shocks. This extraordinarily high level of interconnectedness indicates that regional inflation dynamics are fundamentally interdependent rather than driven primarily by local idiosyncratic factors. The magnitude of this interconnectedness exceeds that typically observed in international spillover studies, suggesting that subnational regions within Peru are more tightly integrated than many sovereign economies.

The directional spillover analysis reveals a pronounced hierarchy in regional influence that fundamentally shapes Peru's inflation landscape. Lima emerges as the overwhelmingly dominant transmitter of inflationary shocks, with TO spillovers of 100.43 percentage points-statistically significant at the 1% level and substantially exceeding all other regions. This dominance reflects Lima's role as Peru's economic epicenter, concentrating 66.02% of national inflation weight and serving as the primary hub for financial markets, import distribution, and policy transmission.

Following Lima in transmission strength, Regions 7 (Huánuco, Cerro de Pasco, Huancayo) and 4 (Trujillo, Chimbote, Huaraz) exhibit significant spillover transmission with TO values of 84.37 and 83.84 percentage points, respectively. Region 7's influence likely stems from its role as a major agricultural and mining center that supplies both Lima and other regions, while Region 4's industrial base and coastal location position it as a secondary distribution hub. In stark contrast, Regions 8 (tourism and mining in the south) and 9 (Amazon regions) contribute minimal spillovers to the system, with TO values of only 39.30 and 46.54 percentage points, reflecting their peripheral economic positions.

The FROM spillover estimates reveal relatively uniform exposure to external shocks across regions, with most regions showing FROM values between 68% and 78%. This homogeneity suggests that while transmission capacity varies dramatically across regions, vulnerability to external spillovers is more evenly distributed. The slight variation that does exist shows Regions 8 and 6 as somewhat less exposed (61.93% and 68.37% respectively), possibly reflecting their greater economic isolation or specialized sectoral focus.

The NET spillover measures reveal stark asymmetries in regional roles within Peru's inflation transmission network. Lima stands out as the dominant net transmitter with a statistically significant NET spillover of 23.94 percentage points-a magnitude that exceeds the combined net transmission of all other positive NET regions. This extraordinary centrality confirms Lima's structural role as the primary source of systematic inflation pressures throughout Peru's regional system.

Region 7 emerges as the only other statistically significant net transmitter (8.87 percentage points), reflecting its important role as an agricultural and mining hub that influences food and commodity prices nationwide. Several regions ($2, 3, 4, 5$, and 6) show small positive or near-zero NET spillovers that are not statistically significant, indicating balanced transmission-reception roles.

On the receiving side, Regions 8 and 9 emerge as significant net recipients with NET spillovers of -22.62 and -24.87 percentage points, respectively, both statistically significant at the 1% level. These regions' consistent absorption of external shocks without corresponding transmission capacity underscores their peripheral status in Peru's economic geography. Region 8's net reception likely reflects its tourism-dependent economy's vulnerability to external conditions,

while Region 9's Amazonian location creates dependence on supply chains from other regions without generating reciprocal influence.

Table 5 presents pairwise net spillovers, computed as the difference between bidirectional spillovers for each region pair. This granular analysis reveals that Lima transmits net shocks to all other regions without exception, with the entire Lima column showing positive and statistically significant values. Lima's most pronounced bilateral influence occurs with Region 9 (5.09 percentage points) and Region 8 (4.76 percentage points), both significant at the 1% level, demonstrating Lima's particular importance for Peru's most peripheral regions that lack alternative inflation anchors.

The bilateral analysis confirms that Regions 8 and 9 are systematically positioned as net recipients across most regional pairs. Their rows contain predominantly positive and significant entries, indicating consistent exposure to spillovers from other regions without reciprocal transmission capacity. This pattern reinforces their structural role as inflation absorbers within Peru's regional network.

Table 5: Time domain pairwise net spillovers

	Lima	Region 2	Region 3	Region 4	Region 5	Region 6	Region 7	Region 8	Region 9
Lima	-								
Region 2	2.26***	-							
Region 3	2.25**	-0.35	-						
Region 4	2.42***	-0.36	-0.05	-					
Region 5	2.59***	-0.29	-0.39	0.53	-				
Region 6	2.22**	0.34	-0.22	0.96	0.80	-			
Region 7	2.34***	-0.66	0.40	-0.23	-0.18	-1.21	-		
Region 8	4.76***	1.43*	1.23	3.04***	2.89*	4.06*	6.47***	-	
Region 9	5.09***	2.26**	1.55	3.07***	3.76***	5.01***	2.88***	1.25	-

Note: This table reports the time domain pairwise net spillovers and its statistical significance: *** significant at the 1% level, ** at the 5% level, and * at the 10% level.

4.1.2 Dynamic Inflation Spillovers: Rolling-Window Analysis

To examine the temporal evolution of spillover relationships and assess their stability across different economic episodes, we implement a rolling-window estimation procedure following Diebold and Yilmaz (2012). Spillover indicators are computed using one-lag VAR and three-month forecast horizon with a rolling window of 150 observations, enabling analysis of evolving patterns from May 2014 through December 2024. We construct 95% confidence intervals using a pivot bootstrap procedure with 5,000 simulations following Choi and Shin (2020), providing formal statistical inference for time-varying spillover dynamics.

Figure 2 illustrates the evolution of the Total Spillover Index across the sample period, revealing significant temporal variation around a high baseline level of interconnectedness. Over the sample period (May 2014-December 2024), the TSI fluctuates between 67.81% and 75.95%, indicating persistently high regional interdependence with meaningful cyclical variation. This range demonstrates that while Peru's regions remain fundamentally interconnected, the intensity of spillover relationships responds systematically to economic conditions and external shocks.

Between May 2014 and February 2020, the TSI remained relatively stable within a narrow band of 73.31% to 75.95%, suggesting robust baseline interconnectedness during normal economic conditions. This stability indicates that Peru's regional inflation transmission mechanisms operated consistently during the pre-pandemic period, providing a reliable foundation for monetary policy transmission.

The most dramatic evolution in spillover connectivity coincides with Peru's COVID-19 response, beginning with a sharp decline from March 2021 and reaching a trough of 67.81% in June 2021. This substantial drop in regional connectivity-a decline of over 8 percentage points from pre-pandemic levels-coincides with Peru's implementation of one of Latin America's most stringent lockdown regimes. Peru declared a national state of emergency on March 15,2020, enforcing strict mobility restrictions that severely limited interregional travel and economic activity, with a second nationwide lockdown introduced in January 2021.

The spillover disruption reflects the breakdown of normal economic transmission channels during the pandemic. Peru's GDP contracted by 11.1% in 2020—the largest annual decline since 1989—reflecting a breakdown in normal economic transmission channels during the pandemic. Nearly all regions experienced significant downturns, with Moquegua showing relative resilience due to sustained mining activity. The most severely affected regions included Pasco (-50.7%),

Madre de Dios (-42.8%), and Arequipa (-32.7%), illustrating how the pandemic created asymmetric regional impacts that temporarily decoupled normal spillover relationships.

From the second half of 2021 onward, the TSI exhibits a gradual but sustained recovery, rising from 67.81% in June 2021 to 74.40% in December 2022. This recovery trajectory closely tracks Peru's economic rebound and the progressive relaxation of mobility restrictions throughout 2021, with complete removal of all restrictions by February 2022. The spillover recovery demonstrates the resilience of Peru's underlying regional economic linkages once normal economic activity resumed.

Beginning in January 2023, the TSI resumed a downward trajectory, falling to 71.74% by June 2023 and remaining stable thereafter between 71.20% and 72.43% through December 2024. This decline and subsequent stabilization occurred alongside a marked deceleration in national inflation, which fell from 8.55% in 2022-the highest since 1996-to 3.38% in 2023 and further to 1.90% in 2024. Notably, the TSI levels during 2023-2024 remain below pre-pandemic levels, suggesting a potential structural shift in regional transmission mechanisms or a new equilibrium in spillover relationships.

These time-varying dynamics in regional inflation spillovers engage with recent findings in the literature on inflation connectedness. Pham and Sala (2022), using data from G7 economies and Spain, show that volatility spillovers tend to intensify during periods of macroeconomic turmoil. By contrast, our results reveal a significant drop in Peru's TSI following nationwide mobility restrictions, suggesting that regional fragmentation in emerging economies may temporarily disrupt transmission channels. Meanwhile, Alqaralleh et al. (2025) find that inflation spillovers are significantly stronger during high-inflation regimes in European economies, consistent with our observation of heightened regional connectedness in 2022 when domestic inflation peaked, followed by a decline as national inflation returned to its target range in 2023–2024.

Figure 3 depicts the time-varying behavior of directional spillovers TO all other regions for each Peruvian region, revealing distinct patterns in regional influence over time. Lima consistently maintains its position as the dominant transmitter throughout the sample period, with its TO spillovers showing an upward trend that becomes particularly pronounced after 2021. This intensification in Lima's transmission capacity during the post-pandemic recovery underscores its growing systemic importance in Peru's regional inflation network.

In contrast, Regions 8 and 9 consistently rank as the least influential transmitters, with their spillover indices remaining relatively low and stable over time. This persistent pattern confirms their structural role as spillover recipients rather than transmitters, maintaining their peripheral status throughout various economic cycles.

A notable structural shift appears in Region 6 (Arequipa, Moquegua, Tacna, Puno), which experiences a marked decline in its TO spillover index around 2020 that persists thereafter. This discontinuity may reflect fundamental changes in the region's economic structure or integration patterns, possibly linked to mining sector developments or trade relationship shifts.

Figure 4 illustrates the dynamics of spillovers FROM all other regions, showing relatively more homogeneous patterns across regions compared to the TO dynamics. The FROM indicators remain relatively stable over time for most regions, suggesting that while transmission capacity varies significantly across regions and time, vulnerability to external spillovers exhibits greater stability.

Figure 2: Dynamic total spillover index in the time domain

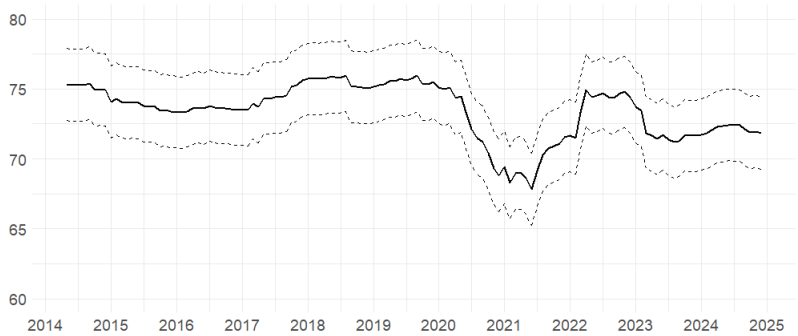

Note: This figure displays the evolution of the Total Spillover Index (TSI) over time, estimated using a rolling window of 150 observations. The dashed lines represent the 95% confidence interval obtained via pivot bootstrap simulations, following the methodology of Choi and Shin (2020).

Figure 3: Dynamic spillovers TO all others in the time domain

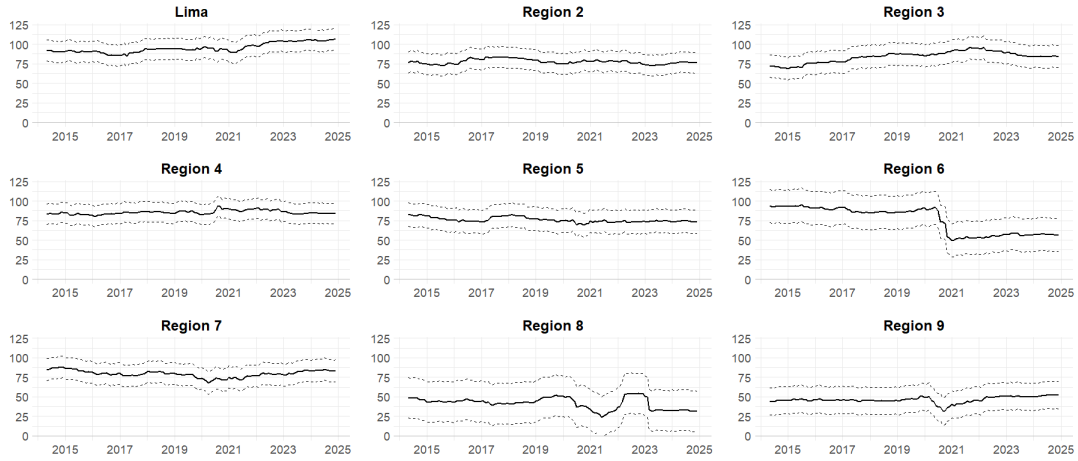

Note: This figure displays the evolution of *TO* directional spillovers over time, estimated using a rolling window of 150 observations. The dashed lines represent the 95% confidence interval obtained via pivot bootstrap simulations, following the methodology of Choi and Shin (2020).

Figure 4: Dynamic spillovers FROM all others in the time domain

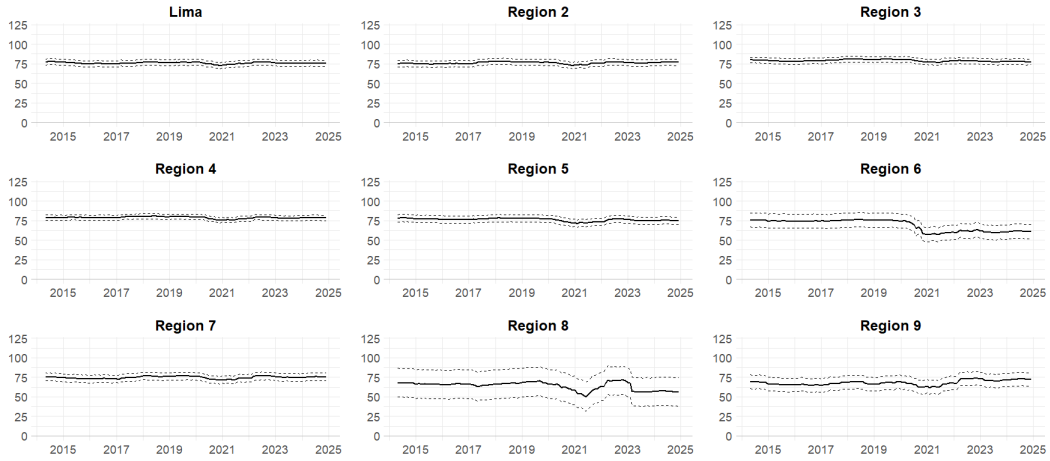

Note: This figure displays the evolution of *FROM* directional spillovers over time, estimated using a rolling window of 150 observations. The dashed lines represent the 95% confidence interval obtained via pivot bootstrap simulations, following the methodology of Choi and Shin (2020).

Figure 5 presents the evolution of NET inflation spillovers across regions, providing crucial insights for monetary policy design. Consistent with static results, Lima emerges as the dominant net transmitter throughout the entire sample period, with its net spillover index exhibiting a clear upward trajectory and particularly pronounced increases following the COVID-19 pandemic. This strengthening trend suggests that Lima's role as Peru's inflation anchor has intensified over time, providing empirical support for the BCRP's continued reliance on Lima's CPI.

Regions 8 and 9 consistently appear as net receivers throughout most of the sample, with negative net spillover indices persisting across different economic conditions. This stability in their recipient roles underscores the importance of considering regional spillover effects when designing monetary policy, as these regions systematically absorb inflationary pressures generated elsewhere in the system.

For the remaining regions, no consistent dominance as net transmitters or receivers emerges over time, indicating relatively balanced positions in terms of inflation transmission and reception. This pattern suggests that most regions play dual roles as both sources and destinations of spillover effects, contributing to the overall interconnectedness of Peru's regional inflation system.

These dynamic spillover patterns provide essential insights for monetary policy implementation, demonstrating that while the fundamental structure of regional relationships remains stable, the intensity of transmission varies meaningfully with economic conditions. The COVID-19 episode, in particular, illustrates both the vulnerability of

spillover mechanisms to severe external shocks and their capacity for recovery once normal economic conditions are restored.

Figure 5: Dynamic NET spillovers in the time domain

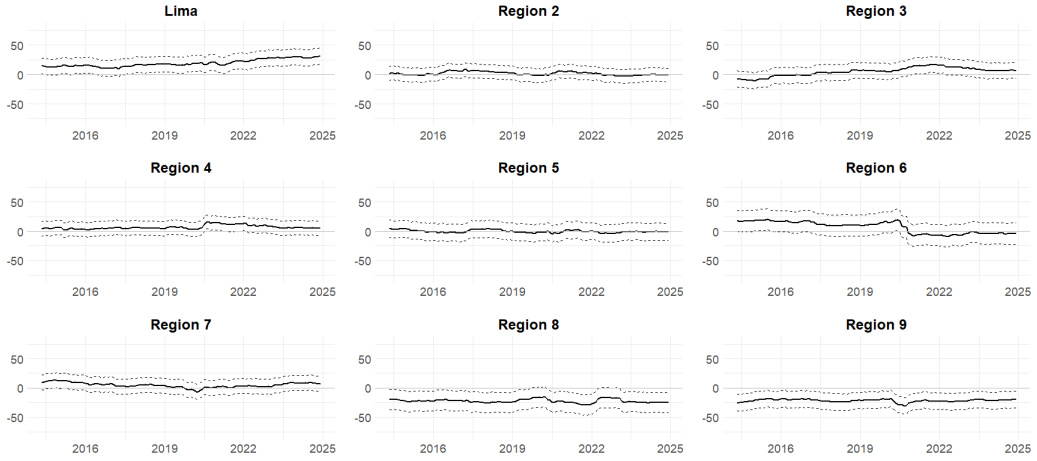

Note: This figure displays the evolution of *NET* directional spillovers over time, estimated using a rolling window of 150 observations. The dashed lines represent the 95% confidence interval obtained via pivot bootstrap simulations, following the methodology of Choi and Shin (2020).

4.2 Frequency-domain spillovers

To complement the time-domain analysis and provide deeper insights into the cyclical nature of regional inflation transmission, we employ the frequency-domain connectedness framework developed by Baruník and Křehlík (2018). This spectral approach enables decomposition of spillovers across different cyclical horizons, distinguishing between short-term fluctuations driven by transitory supply shocks and long-term persistence reflecting structural economic relationships—a distinction crucial for understanding the temporal architecture of Peru's regional inflation dynamics and designing optimal monetary policy responses. Specifically, we partition the spectrum into two distinct bands: the first, $(\pi, \pi/3)$, captures short-term movements, while the second, $(\pi/3, 0)$, reflects longer-term interactions.[4] The short-run band $(\pi, \pi/3)$ corresponds to cyclical behaviors with periodicities ranging from 2 to 6 months.[5] The complementary band $(\pi/3, 0)$ encompasses lower-frequency components with periodicities exceeding 6 months, allowing us to isolate medium- and long-run fluctuations associated with persistent inflation behavior.[6] As with the Diebold–Yilmaz framework, we conduct both static and time-varying estimations using a rolling-window approach.

[4]In the frequency-domain analysis of real-valued time series, the spectral density is symmetric around zero. Specifically: (i) negative frequencies (from $-\pi$ to 0) provide no additional information beyond what is captured by the positive frequencies (from 0 to π); and (ii) this symmetry derives from the property that the Fourier transform of a real-valued signal satisfies the complex conjugate relationship $S(-\omega) = \overline{S(\omega)}$. As a result, bands such as $(\pi, \pi/3)$ and $(\pi/3, 0)$ implicitly reference only the positive half of the spectrum, with the understanding that the negative side is its mirror image. While many empirical implementations of Baruník and Křehlík (2018) adopt a two-band structure to delineate transitory and persistent dynamics, the framework itself allows for arbitrarily refined spectral segmentation. This flexibility enables richer characterizations of cyclical behavior, including the identification of medium-term regimes—an extension we incorporate in our frequency decomposition.

[5]This mapping arises from the angular frequency–period relationship $T = 2\pi/\omega$, which links angular frequency ω (in radians per time unit) to the cycle length T. At the upper boundary, $\omega = \pi$ yields $T = 2$ months—the shortest detectable cycle under the Nyquist limit for discrete monthly data. Frequencies exceeding π radians/sample are subject to aliasing and cannot be reliably interpreted. At the lower boundary, $\omega = \pi/3$ corresponds to $T = 6$ months, marking the upper edge of high-frequency variation. Accordingly, the interval $(\pi, \pi/3)$ captures short-term inflation dynamics with periodicities between 2 and 6 months, while cycles shorter than 2 months are excluded by construction. Tiwari et al. (2019) adopt a spectral decomposition into the bands $(\pi, \pi/4)$ and $(\pi/4, 0)$, which they associate with horizons of up to four months and beyond, respectively. Although our frequency band structure mirrors theirs formally, the interpretation of $\pi/4$ as implying a four-month cycle is inconsistent with the standard frequency–period identity. Specifically, $\omega = \pi/4$ corresponds to a cycle length of eight months. This discrepancy likely reflects a textual simplification rather than a methodological flaw, as their framework remains structurally compatible with established spectral analysis.

[6]Following Martins and Verona (2021), who partition inflation dynamics into frequency bands to distinguish between transitory and structural patterns, we adopt $(\pi, \pi/3)$ as the short-run interval to enhance the separation between high-frequency shocks and deeper, persistent trends. Martins and Verona argue that energy inflation and temporary supply disruptions dominate this high-frequency range, while cycles beyond 6 months increasingly reflect underlying structural forces—supporting the use of a 6-month threshold as a more precise delineation of short-run inflation behavior.

4.2.1 Static Inflation Spillovers

We begin by presenting the static results, which summarize the spillover patterns across frequency bands over the full sample period. Table 6 reports the estimated inflation spillovers across regional units, derived from the frequency-domain connectedness framework. In line with the time-domain analysis, and following Patton (2013) and Fousekis and Tzaferi (2021), we evaluate the statistical significance of the spillover measures using a Wald-type test. The test statistic is computed based on a covariance matrix constructed from 5,000 bootstrap replications.

As a first result, the frequency-specific spillover index (FSI) in the long-run band is markedly higher (44.70) than in the short-run band (28.99), indicating that inflation interdependence across regions is more pronounced at lower frequencies. This suggests that persistent, structural forces—rather than short-lived shocks—are the primary drivers of inflation spillovers within the Peruvian economy.

In the high-frequency band, the spillover architecture reveals a markedly different pattern from both the time-domain results and our conventional understanding of Lima's role. Most strikingly, Lima does not exhibit statistically significant net spillover transmission in the short-run spectrum (NET=-3.24, significant at 10% level as a net recipient), contrasting sharply with its dominance in aggregate time-domain analysis. Instead, Regions 3 (Chiclayo, Cajamarca, Chachapoyas) and 7 (Huánuco, Cerro de Pasco, Huancayo) emerge as the primary short-run transmitters, with statistically significant NET spillovers of 6.51 and 4.89 percentage points, respectively. This pattern reflects these regions' roles as key contributors of agricultural staples and mining outputs that fuel short-run price dynamics across the national inflation network. Region 8 emerges as a significant net recipient in the short-run band (NET=-5.37, significant at 5% level), consistent with its tourism-dependent economy's vulnerability to external price shocks without corresponding capacity to influence other regions' price dynamics over immediate horizons. The relatively balanced spillover relationships among other regions suggest that short-run inflation transmission exhibits greater symmetry and bidirectional flows compared to the hierarchical structure observed at longer horizons.

The long-run frequency band reveals a dramatically different spillover configuration that closely mirrors the time-domain findings. Lima reemerges as the overwhelmingly dominant net transmitter with a NET spillover of 27.23 percentage points-statistically significant at the 1% level and representing the largest regional influence in the entire frequency decomposition. This long-run dominance reflects Lima's structural role in Peru's economy: monetary policy transmission originates from the capital's financial markets, aggregate demand pressures emanate from its concentrated economic activity, and macroeconomic shocks diffuse outward through established commercial and financial networks. The magnitude of Lima's long-run transmission (TO = 65.70 percentage points) substantially exceeds its short-run influence (TO = 34.81 percentage points), demonstrating that Lima's systemic importance materializes primarily through persistent, structural channels rather than immediate supply relationships. This finding has profound implications for monetary policy design, suggesting that while Lima may be vulnerable to short-term supply shocks from other regions, its role as an inflation anchor operates primarily through long-term expectation formation and structural price determination.

Regions 8 and 9 maintain their roles as significant net recipients in the long-run band, with NET spillovers of -17.07 and -24.29 percentage points, respectively, both statistically significant. However, their long-run absorption of spillovers occurs through different mechanisms than short-run reception: rather than immediate supply chain vulnerabilities, their long-run recipient status reflects structural economic dependence on price trends determined in Lima and other economic centers, transmitted through wage indexation, service pricing, and gradual adjustment of local price levels to national trends.

The frequency decomposition reveals several regions that fundamentally change their spillover roles across cyclical horizons, providing insights into the complex temporal structure of regional inflation transmission. Region 3 transforms from a significant shortrun transmitter $(\text{NET} = 6.51)$ to a modest long-run recipient (NET = -6.02), illustrating how agricultural regions can drive immediate price pressures while remaining structurally dependent on broader economic trends for sustained inflation dynamics. Region 6 (Arequipa, Moquegua, Tacna, Puno) exhibits the opposite transformation: relatively passive in short-run dynamics (NET = -4.62) but emerging as a moderate longrun transmitter (NET= 8.80). This pattern likely reflects the region's mining and industrial base, which influences long-term price trends through investment cycles and commodity market integration while remaining less influential in immediate supply chain dynamics. These role reversals across frequencies demonstrate the importance of frequency-domain analysis for understanding regional monetary transmission. Traditional time-domain approaches aggregate these contrasting dynamics, potentially obscuring the distinct mechanisms through which different regions influence national inflation at various temporal horizons.

The pairwise net spillovers across frequencies, presented in Table 7, broadly reflect the aggregate transmission patterns discussed earlier, while providing a more granular view of bilateral inflation dynamics across distinct cyclical horizons. In the short-run band, spillover relationships remain relatively balanced and bidirectional among most regional pairs.

Notably, Lima registers statistically significant net spillovers from multiple regions, including Regions 3, 4, and 7. These short-run transmissions likely reflect direct supply chain linkages—such as harvest variability, weather-induced production shocks, logistical bottlenecks, and commodity price volatility—that quickly propagate through retail markets. This pattern reinforces Lima's role as a short-run recipient of supply-driven price pressures originating in upstream producing regions.

The long-run bilateral relationships reveal a markedly hierarchical structure with Lima transmitting significant net spillovers to nearly all other regions. Lima's bilateral influence is particularly pronounced with peripheral regions: 4.91 percentage points to Region 9 and 4.19 percentage points to Region 8, both statistically significant. This systematic pattern demonstrates that Lima's structural influence operates through persistent, broad-based transmission to all regions rather than concentrated effects on specific regional partners.

Table 6: Frequency domain spillovers

	Lima	Region 2	Region 3	Region 4	Region 5	Region 6	Region 7	Region 8	Region 9	FROM
Short run: Bands (π - $\frac{\pi}{3}$)										
Lima	11.85	5.74	6.41	6.69	5.53	2.99	6.50	1.07	3.11	38.04***
Region 2	5.34	12.59	7.02	7.22	3.84	3.02	4.80	1.09	3.11	35.43***
Region 3	4.82	5.57	10.48	5.21	3.05	2.03	4.26	0.95	2.64	28.55***
Region 4	5.80	6.33	5.80	11.57	4.31	2.70	5.16	1.24	2.70	34.06***
Region 5	5.17	3.73	3.61	4.54	10.88	2.53	4.39	1.38	3.13	28.47***
Region 6	3.64	3.88	3.03	3.61	3.26	12.45	3.25	4.05	2.17	26.89***
Region 7	5.01	4.18	4.43	4.87	3.99	2.43	10.10	1.57	2.77	29.25***
Region 8	1.70	1.63	1.35	1.85	1.96	4.93	2.67	15.66	1.78	17.87***
Region 9	3.31	3.40	3.41	3.09	3.28	1.62	3.12	1.14	13.37	22.38***
TO	34.81***	34.47***	35.06***	37.07***	29.22***	22.26***	34.14***	12.50***	21.42***	
NET	-3.24	-0.96	6.51***	3.01	0.75	-4.62	4.89*	-5.37**	-0.96	**FSI = 28.99*** **
Long run: Bands ($\frac{\pi}{3}$ - 0)										
Lima	11.64	4.67	5.46	5.65	6.93	5.21	5.20	1.83	3.52	38.47***
Region 2	7.35	11.42	6.44	6.23	4.95	5.31	4.43	1.59	4.26	40.55***
Region 3	9.31	7.50	11.26	7.07	6.50	5.76	5.98	3.20	4.39	49.71***
Region 4	8.97	6.74	6.44	9.92	6.12	5.08	6.04	1.93	3.13	44.45***
Region 5	9.87	4.71	5.51	6.40	12.93	6.23	7.06	3.93	4.01	47.72***
Region 6	6.72	4.69	4.44	5.07	6.23	19.11	6.21	7.07	1.13	41.56***
Region 7	9.03	4.33	6.19	6.08	7.29	5.83	14.36	4.40	3.14	46.29***
Region 8	6.02	2.40	4.03	4.34	6.24	10.10	9.87	22.15	1.32	44.32***
Region 9	8.43	6.20	5.19	5.81	7.69	6.84	5.72	3.31	15.06	49.19***
TO	65.70***	41.24***	43.69***	46.65***	51.94***	50.36***	50.51***	27.25***	24.91***	
NET	27.23***	0.69	-6.02	2.21	4.23	8.80	4.23	-17.07**	-24.29***	**FSI = 44.70*** **

Note: This table reports the spillovers in the frequency domain. For the FSI, TO, FROM and NET spillovers measures, we report its statistical significance: *** significant at the 1% level, ** at the 5% level, and * at the 10% level.

4.2.2 Dynamic Inflation Spillovers: Rolling-Window Analysis

To examine the temporal evolution of frequency-specific spillovers, we implement rolling-window estimation using 150-observation windows with bootstrap confidence intervals. For each window, connectedness measures are computed separately for the short-run $(\pi, \frac{\pi}{3})$ and long-run $(\frac{\pi}{3}, 0)$ frequency bands. Confidence intervals at the 95% level are constructed via pivot bootstrap with 5,000 replications, following the procedure outlined by Choi and Shin (2020). Figure 6 displays the dynamic evolution of frequency-specific spillover indices, confirming that the FSI remains substantially higher at longer horizons throughout the sample period while revealing important cyclical variations in both frequency bands.

The short-run FSI exhibits notable within-sample variation, following an upward trajectory from May 2014 to February 2020 (rising from 25.64% to 34.41%) that intensifies following COVID-19 mobility restrictions, peaking at 37.48% in June 2021. This increase in short-run connectedness during the pandemic likely reflects synchronized retail price adjustments triggered by supply chain fragmentation, panic purchasing behavior, and logistical disruptions affecting agricultural product flows from producing regions to urban markets.

The intensification of short-run spillovers during crisis periods demonstrates how supply chain vulnerabilities can temporarily amplify immediate price transmission relationships. Food staples like potatoes, onions, and legumes faced transportation constraints and irregular distribution, causing retail markets across regions-particularly Lima-to respond in unison to supply disruptions, thereby strengthening short-term comovements in inflation.

Table 7: Frequency domain pairwise net spillovers

	Lima	Region 2	Region 3	Region 4	Region 5	Region 6	Region 7	Region 8	Region 9
Short run: Bands (π - $\frac{\pi}{3}$)									
Lima	-								
Region 2	-0.40	-							
Region 3	-1.59***	-1.44***	-						
Region 4	-0.89*	-0.88*	0.59	-					
Region 5	-0.36	-0.10	0.56*	0.22	-				
Region 6	0.65	0.86	1.00**	0.91*	0.73*	-			
Region 7	-1.48***	-0.62	0.16	-0.29	-0.40	-0.82*	-		
Region 8	0.63	0.54	0.40	0.60*	0.58	0.88	1.10***	-	
Region 9	0.20	0.29	0.77	0.39	0.15	-0.55	0.35	-0.64	-
Long run: Bands ($\frac{\pi}{3}$ - 0)									
Lima	-								
Region 2	2.68***	-							
Region 3	3.85***	1.06	-						
Region 4	3.31***	0.51	-0.63	-					
Region 5	2.94***	-0.24	-1.00	0.28	-				
Region 6	1.52	-0.62	-1.32	-0.01	0.00	-			
Region 7	3.83***	-0.10	0.21	0.04	0.23	-0.38	-		
Region 8	4.19***	0.81	0.83	2.41**	2.31	3.03	5.47***	-	
Region 9	4.91***	1.94*	0.80	2.68***	3.67***	5.71***	2.58**	1.99*	-

Note: This table reports the frequency domain pairwise net spillovers and its statistical significance: *** significant at the 1% level, ** at the 5% level, and * at the 10% level.

The long-run FSI follows a distinct evolutionary pattern that more closely mirrors the time-domain results. Between May 2014 and February 2020, long-term connectedness remained relatively stable between 43.11% and 48.35%. However, following COVID-19 mobility restrictions, the long-run index declined sharply to 30.36% in June 2021, reflecting temporary weakening of structural inflation linkages as regional economies underwent asynchronous adjustments to pandemic shocks.

The breakdown of long-run spillovers during the pandemic reflects disruption of fundamental transmission mechanisms: inter-regional labor mobility declined, investment linkages weakened, and financial market integration temporarily fragmented. The subsequent recovery to 42.57% by April 2022 coincides with the 2022 inflationary surge driven by global commodity shocks, exchange rate pass-through, and nationwide monetary responses-macroeconomic pressures that reactivated structural spillover mechanisms.

Having established the contrasting evolution of aggregate spillover intensity across frequencies, we now turn to the directional dynamics underlying these patterns. Specifically, we examine how individual regions contribute to and receive inflationary pressures over time, and whether these roles differ across cyclical horizons. This disaggregated analysis offers a more nuanced view of inflation transmission mechanisms, highlighting both symmetrical and asymmetrical relationships across Peru's regional landscape.

Figures 7 and 8 illustrate the evolution of TO spillovers across frequency bands, revealing distinct temporal patterns. Lima's short-term transmission capacity remains relatively stable and consistently below its long-term influence throughout the sample period. In contrast, Lima's long-run TO spillovers exhibit a clear upward trend, particularly pronounced following the pandemic, reinforcing its growing structural centrality in Peru's inflation network. Regions 8 and 9 consistently display the lowest TO values across both frequency bands and throughout time, confirming their persistent peripheral status regardless of cyclical horizon. However, their spillover reception patterns (Figures B1 and B2 in appendix) show greater stability in the long-run band, suggesting that while their immediate supply chain vulnerabilities may fluctuate, their structural dependence on external price determination remains consistent.

The NET spillover profile highlights the transmission asymmetries observed in the TO analysis, summarizing each region's net position over time. As shown in Figures 9 and 10, which depict short- and long-term NET dynamics,

Figure 6: Dynamic frequency spillover index in the frequency domain

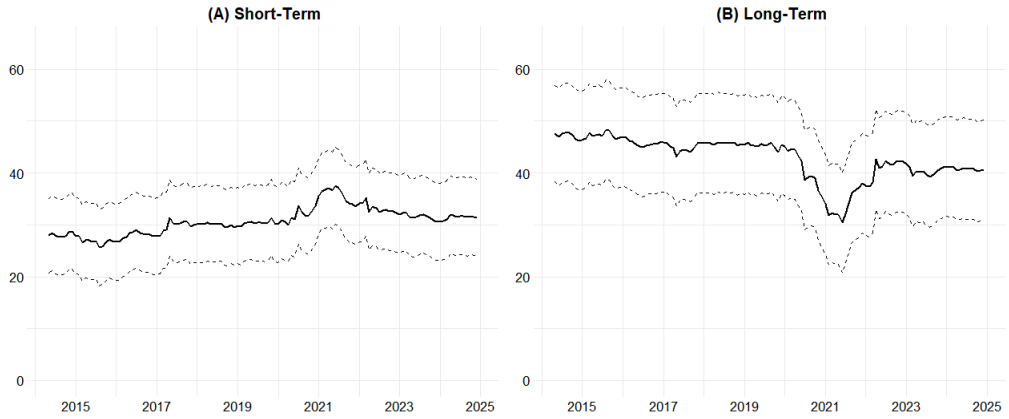

Note: This figure displays the evolution of the Frequency Spillover Index (FSI) over time, decomposed across different frequency bands , estimated using the BK methodology (Baruník and Křehlík, 2018). The analysis is based on a rolling window of 150 observations. Panel A shows short-term connectedness, corresponding to the frequency band $(\pi, \frac{\pi}{3})$, while Panel B shows long-term connectedness, associated with the band $(\frac{\pi}{3}, 0)$. The dashed lines represent 95% confidence intervals obtained through 5,000 pivot bootstrap simulations, following the methodology of Choi and Shin (2020).

respectively, short-run values remain relatively stable across all regions, with no clear evidence of sustained net transmitters or receivers. Lima does not exhibit a dominant short-run net position, and overall dynamics at high frequencies appear comparatively symmetric across regions. In contrast, long-term NET spillovers reveal stronger cross-regional variation. Lima emerges as the primary net transmitter of inflation, with a noticeable upward trend in its long-run NET values over the sample period. Conversely, Regions 8 and 9 consistently register negative long-term NET values, underscoring their role as structural net recipients of inflationary pressures.

The dynamic frequency-domain analysis provides crucial insights for monetary policy implementation during different phases of economic cycles. The temporary intensification of short-run spillovers during crisis periods suggests that immediate policy responses should account for amplified supply chain transmission, while the resilience of long-run structural relationships validates Lima's continued role as a reliable inflation anchor during normal economic conditions.

The contrasting behavior of spillovers across frequencies during the 2022 inflationary episode-where long-run connectedness strengthened while short-run spillovers moderated—demonstrates that different temporal horizons of spillover relationships respond distinctly to various types of economic shocks. This frequency-dependent responsiveness underscores the value of the spectral approach for understanding the complex temporal architecture of regional inflation transmission and designing horizonspecific policy responses.

Figure 7: Dynamic TO spillovers to all others in the short run

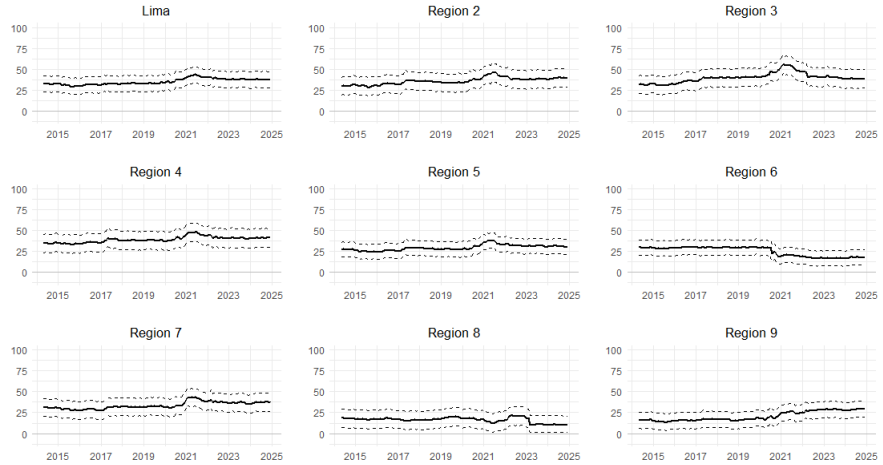

Note: This figure shows the short-term TO spillovers $(\pi, \frac{\pi}{3})$, estimated using the BK methodology (Baruník and Křehlík, 2018). Results are based on a rolling window of 150 observations. Dashed lines indicate 95% confidence intervals from 5,000 pivot bootstrap simulations (Choi and Shin, 2020).

Figure 8: Dynamic TO spillovers to all others in the long run

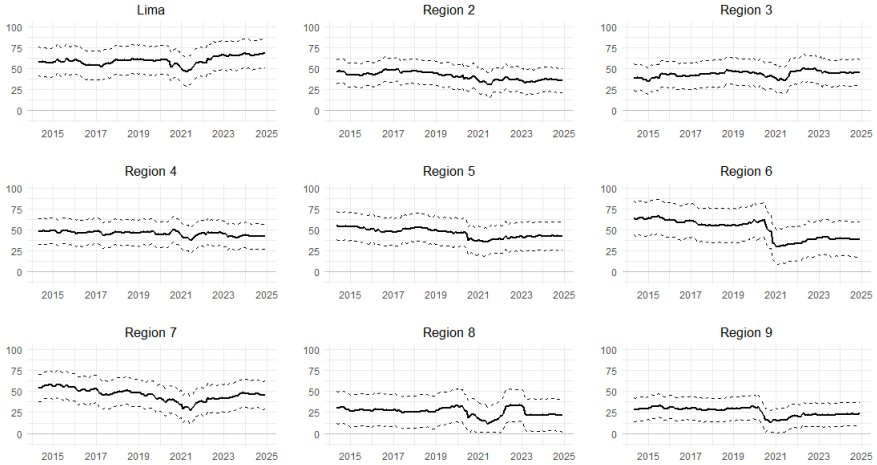

Note: This figure shows the long-term TO spillovers ($\frac{\pi}{3}$, 0), estimated using the BK methodology (Baruník and Křehlík, 2018). Results are based on a rolling window of 150 observations. Dashed lines indicate 95% confidence intervals from 5,000 pivot bootstrap simulations (Choi and Shin, 2020).

Figure 9: Dynamic NET spillovers in the short run

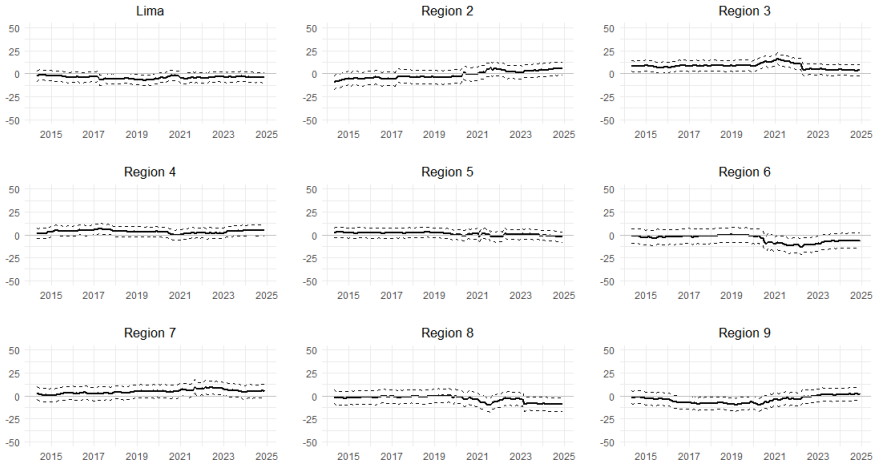

Note: This figure shows the short run NET spillovers (π , $\frac{\pi}{3}$), estimated using the BK methodology (Baruník and Křehlík, 2018). Results are based on a rolling window of 150 observations. Dashed lines indicate 95% confidence intervals from 5,000 pivot bootstrap simulations (Choi and Shin, 2020).

Figure 10: Dynamic NET spillovers in the long run

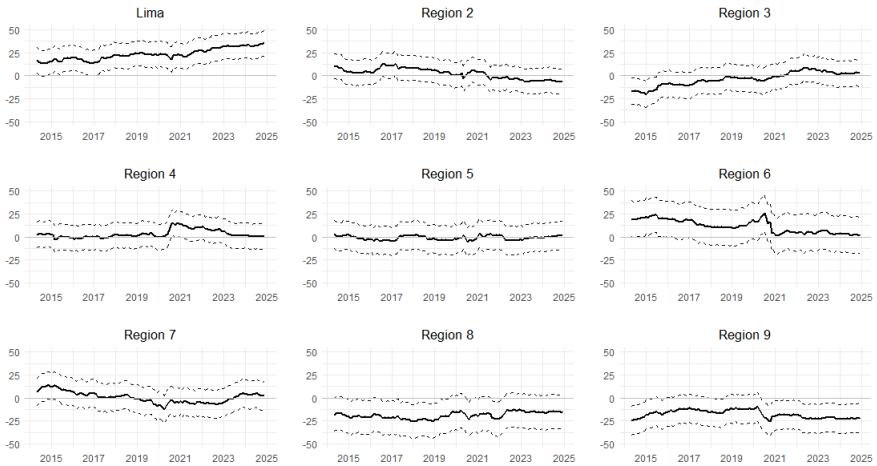

Note: This figure shows the long-term NET spillovers ($\frac{\pi}{3}$, 0), estimated using the BK methodology (Baruník and Křehlík, 2018). Results are based on a rolling window of 150 observations. Dashed lines indicate 95% confidence intervals from 5,000 pivot bootstrap simulations (Choi and Shin, 2020).

4.3 Robustness Analysis

To ensure the reliability and generalizability of our spillover findings, we conduct an extensive robustness analysis that systematically examines the sensitivity of our results across multiple dimensions. Our robustness framework tests the stability of regional spillover patterns under alternative model specifications, temporal aggregations, spatial classifications, and methodological approaches, providing comprehensive validation of our core empirical findings. This multi-faceted approach is essential given the policy importance of our results for Peru's monetary framework and their potential applicability to other emerging economies with similar regional heterogeneity.

Our comprehensive robustness analysis demonstrates remarkable stability in Peru's regional inflation spillover architecture across the multiple dimensions of sensitivity testing we have conducted. Key findings prove robust to: alternative model specifications (forecast horizons, lag lengths), granular city-level analysis, and varying frequency decompositions (two-band vs. three-band).

Most importantly, the core policy-relevant findings remain consistent across all robustness checks: Lima's structural dominance as a long-run inflation transmitter, the frequency-dependent nature of regional spillover relationships, and the persistent peripheral status of remote regions in Peru's spillover network. This robustness provides strong confidence in the policy recommendations derived from our analysis and suggests broad applicability of our methodological framework to other emerging economies with similar regional heterogeneity.

The stability of our findings across diverse specifications also validates the economic interpretations underlying our results: Lima's dominance reflects genuine structural centrality in Peru's economy rather than statistical artifacts, while the frequency-dependent spillover patterns capture real differences between supply-chain transmission (short-run) and monetary policy transmission (long-run) mechanisms. This robustness strengthens the case for continued reliance on Lima's CPI as Peru's inflation-targeting anchor while supporting enhanced attention to frequency-specific regional dynamics in monetary policy implementation.

4.3.1 Time-Domain Robustness Checks

Sensitivity to Model Specification Parameters

We begin by assessing the robustness of time-domain spillover estimates to key methodological choices that could potentially influence our conclusions. Following the approaches of Diebold and Yilmaz (2012), we systematically vary forecast horizons and lag lengths while monitoring the stability of regional spillover rankings and magnitudes.

Table A1 reports the sensitivity of spillover measures to forecast horizon variations, with horizons ranging from $H = 1$ to $H = 12$ months while maintaining a fixed lag length of $L = 1$. Each cell presents the median value across horizons, with minimum and maximum values in brackets to illustrate the range of variation. The results demonstrate remarkable stability in regional spillover hierarchies: Lima consistently emerges as the dominant net transmitter across all forecast horizons, with median NET spillovers of 23.99 percentage points and a narrow range of 11.78 to 24.00 percentage points.

Similarly, Regions 8 and 9 maintain their roles as significant net recipients across all horizons, with relatively narrow ranges around their median values (-22.44 and -25.24 respectively). This consistency demonstrates that our key findings about regional transmission hierarchies are not artifacts of specific forecast horizon choices but reflect robust structural relationships in Peru's regional inflation network.

Table A2 examines sensitivity to VAR lag length specifications, varying from $L = 1$ to $L = 6$ while holding the forecast horizon constant at $H = 3$. The results confirm the robustness of our spillover rankings, with Lima's median NET spillover of 20.00 percentage points remaining substantially above all other regions across all lag specifications. The stability of these patterns suggests that our findings capture genuine economic relationships rather than statistical artifacts of particular model specifications.

Dynamic Robustness Assessment

To assess the stability of our dynamic spillover estimates, we implement rolling-window analysis across forecast horizons $\mathrm{H} = 1$ to $\mathrm{H} = 12$. Figure B3 illustrates the evolution of NET spillovers, with the solid black line denoting the median trajectory across horizons and the shaded area capturing the full range between minimum and maximum estimates.

Lima's dynamic NET spillover evolution shows remarkable consistency, with the median closely tracking the upper bound throughout the sample period. This pattern reflects Lima's persistently strong transmission role across different forecast horizons. Notably, Lima's spillover intensity increases with horizon length, as evidenced by the lower bound

(corresponding to $H = 1$ and $H = 2$) remaining substantially below the median. This horizon-dependent strengthening provides empirical support for our frequency-domain analysis, which explicitly demonstrates Lima's greater influence at longer cyclical periods.

Figures B4 and B5 present additional robustness checks examining sensitivity to lag length specifications ($L = 1$ to $L = 6$) and rolling window sizes (100, 150, and 200 observations), respectively. Figure B4 illustrates the evolution of NET spillovers, with the solid black line denoting the median trajectory across lag specifications and the shaded area capturing the full range between minimum and maximum estimates. Across all variations, the fundamental pattern persists: Lima maintains its dominant net transmitter role, while Regions 8 and 9 consistently appear as net recipients. The stability of these relationships across diverse specifications reinforces confidence in our core empirical findings.

City-Level Granular Analysis

As a comprehensive robustness check, we re-estimate spillover measures using monthly inflation data from Peru's 25 largest cities individually, rather than the nine regional aggregates employed in our main analysis. This granular approach tests whether our findings are sensitive to the spatial aggregation scheme and provides validation using the finest available geographic resolution.

Table A3 presents the city-level spillover results, revealing a total spillover index of 73.68%—virtually identical to our regional aggregate finding of 73.60%.[7] This remarkable consistency demonstrates that our aggregation methodology preserves the essential spillover structure present in the underlying city-level data. Lima emerges as the dominant net transmitter at the city level with a NET spillover of 54.96 percentage points-even more pronounced than in regional analysis, confirming its central role in Peru's spatial inflation network.

Cities corresponding to our peripheral regions (Iquitos, Puerto Maldonado) exhibit the largest negative NET spillovers (-40.00 and -36.18 percentage points), while cities in food-producing regions (Chiclayo, Huancayo) show significant positive transmission. These patterns align precisely with our regional findings, validating both our aggregation methodology and our economic interpretations of regional spillover roles.

4.3.2 Frequency Domain Approach

Alternative Frequency Band Specifications

To ensure our frequency-domain results are not dependent on the specific two-band decomposition employed in our main analysis, we implement a three-band specification following Istiak et al. (2021). This refined decomposition distinguishes between short-term $(\pi, \pi/3)$, medium-term $(\pi/3, \pi/12)$, and long-term $(\pi/12, 0)$ dynamics, corresponding approximately to 2-6 months, 6-24 months, and $24+$ months respectively.

Table A4 presents the three-band decomposition results, confirming and refining our main frequency-domain findings. In the short-term band, Lima appears as a statistically significant net recipient (NET = -3.24, p<0.10), consistent with our two-band analysis. However, the three-band decomposition reveals that Lima's transformation to dominance occurs primarily in the medium-term band (NET = 16.76, p<0.01), with continued strong transmission in the long-term band (NET = 10.48, p<0 .01).

This three-band analysis provides crucial insights into the temporal structure of Lima's influence: its dominance emerges most strongly in the medium-term band (6-24 months), corresponding to monetary policy transmission cycles and business cycle frequencies. The persistence of significant transmission into the longest band (24+ months) confirms Lima's role in long-term inflation anchor formation and structural price determination.

Regions 8 and 9 maintain negative NET spillovers across all three bands, with particularly pronounced medium-term reception (-10.20 and -14.36 percentage points), suggesting that their structural dependence on external price determination operates most strongly at business cycle frequencies.

City-Level Frequency Analysis

We extend our frequency-domain robustness analysis to the city level, implementing the Baruník-Křehlík methodology on all 25 cities for both short-run and long-run bands. Tables 10 and 11 present selected results, confirming our regional frequency patterns at the finest spatial resolution.[8]

In the short-run band (Table A5), Lima shows a modest positive NET spillover (3.14) that is not statistically significant, while cities in agricultural regions (Chiclayo: 10.24, Huancayo: 3.30) exhibit stronger short-run transmission. This

[7] Estimation is based on a VAR model with one lag and a forecast horizon of three months.

[8] Estimation uses a VAR model with one lag and a forecast horizon of three months.

pattern aligns with our regional finding that food-producing areas drive immediate price pressures that subsequently affect Lima.

In the long-run band (Table A6), Lima's dominance becomes overwhelming with a NET spillover of 47.87 percentage points ($p<0.01$)—substantially larger than any other city. Cities corresponding to peripheral regions (Iquitos: -34.20, Puerto Maldonado: -23.93) maintain their recipient roles, while secondary urban centers (Arequipa, Trujillo) show modest transmission capacity.

Dynamic Frequency Robustness

Figure B6 presents the dynamic evolution of NET spillovers across our three-band frequency decomposition, confirming the temporal stability of frequency-dependent regional roles. Lima consistently displays negative NET spillovers in the short-term band throughout the sample period, while maintaining positive and generally increasing NET spillovers in both medium- and long-term bands. This temporal consistency across the entire sample period demonstrates that the frequency-dependent spillover patterns are structural features of Peru's regional economy rather than temporary phenomena.

5 Conclusions and Policy Implications

This study provides robust empirical evidence on the regional architecture of inflation spillovers in Peru, documenting pronounced asymmetries in how inflationary shocks propagate across the country's nine economic regions. Using both time-domain (Diebold-Yilmaz) and frequency-domain (Baruník-Křehlík) methodologies on monthly CPI data from 2002-2024, we establish that Lima consistently emerges as the dominant net transmitter of inflationary shocks (net spillover of 23.94 percentage points), while peripheral regions like Regions 8 and 9 serve as persistent net recipients (net spillovers of -22.62 and -24.87 , respectively).

Our frequency decomposition reveals a striking dual role for Lima in Peru's inflation transmission network. In the short run (2-6 months), Lima functions primarily as a net recipient of inflationary shocks, particularly from food-producing regions (Regions 3 and 7), reflecting its dependence on regional supply chains for essential goods. However, over longer horizons ($6+$ months), Lima consistently emerges as the dominant transmitter, with the longrun frequency-specific spillover index (FSI) reaching 44.70% compared to only 28.99% in the short run. This temporal asymmetry underscores how structural economic forces-monetary policy transmission, aggregate demand dynamics, and macroeconomic fundamentals-mainly originate from the capital and propagate outward over extended periods.

The dynamic evolution of spillovers during COVID-19 mobility restrictions and the 2022 inflationary surge provides crucial insights into crisis management. Short-run spillovers intensified during logistical fragmentation, while long-run spillovers declined and later recovered, illustrating how structural transmission mechanisms can be temporarily disrupted before being reactivated by common macroeconomic pressures. Lima's long-run net spillovers displayed a persistent upward trend, reinforcing its growing centrality in national inflation dynamics.

These findings provide strong empirical validation for the BCRP's continued use of Lima's CPI as the primary inflation-targeting anchor. Lima's structural dominance in long-run spillovers (net spillover of 27.23 percentage points in the long-run frequency band) confirms its suitability as a credible benchmark for national price stability objectives and substantiates the Central Reserve Bank's reliance on Lima's CPI for anchoring inflation expectations. The robustness of these patterns across alternative specifications, spatial aggregation levels, and frequency segmentations demonstrates the reliability of Lima's centrality for operational policy analysis.

However, the frequency-domain analysis suggests concrete enhancements to current policy practice. The BCRP should integrate geographically disaggregated signals from foodproducing regions (Regions 3 and 7) into near-term inflation forecasts. Monthly monitoring systems for agricultural price developments, supply chain tracking mechanisms linking regional disruptions to anticipated Lima price pressures, and weather-indexed forecasting models incorporating climate shocks represent actionable improvements to current forecasting frameworks.

For persistently vulnerable regions (Regions 8 and 9), which consistently absorb long-run inflationary pressures without effective transmission capabilities, targeted stabilization measures merit consideration. Early warning systems linked to Lima's inflation dynamics could enhance regional policy responsiveness. Additionally, our COVID-19 analysis reveals that structural spillover mechanisms can be temporarily disrupted during severe shocks, suggesting the need for adaptive policy responses that account for temporary breakdowns in normal transmission channels, including contingency forecasting models and flexible targeting approaches during crisis periods.

From a theoretical perspective, our findings extend understanding of monetary policy transmission in spatially heterogeneous economies. The documented frequency-dependent spillovers challenge traditional models that assume uniform

policy transmission, suggesting that optimal monetary policy should account for both short-run supply-side shocks from peripheral regions and long-run demand-side transmission from economic centers. This dual-frequency framework provides a more sophisticated foundation for understanding monetary policy effectiveness across space and time, with broader applicability to other emerging economies facing similar center-periphery dynamics.

The methodology developed here-combining time-domain and frequency-domain spillover analysis-offers a generalizable framework for analyzing regional inflation dynamics in spatially diverse economies. Countries like Brazil, India, South Africa, and Mexico face comparable challenges in designing monetary policy for economically heterogeneous regions, and the analytical tools demonstrated here provide practical approaches for addressing these challenges. The frequency-domain extension proves particularly valuable for distinguishing between transitory supply shocks and persistent structural transmission, a distinction crucial for policy design in emerging economies with pronounced regional diversity.

Looking forward, future research should develop time-varying parameter models that endogenously determine optimal regional weights in inflation targeting frameworks, particularly during structural breaks or crisis periods. Cross-country applications of our methodology could establish generalizable principles for regional inflation management, while real-time spillover indices could inform monthly policy decisions through machine learning approaches processing high-frequency regional price data. The intersection of regional inflation spillovers with financial stability concerns represents another promising avenue for investigation.

In synthesis, Lima's dual role as short-run recipient and long-run transmitter of inflation provides a robust empirical foundation for Peru's monetary policy framework that balances national coherence with regional heterogeneity. The Central Reserve Bank of Peru should maintain its Lima-centered inflation targeting approach while enhancing regional monitoring capabilities and crisis preparedness mechanisms. As Peru's economy continues evolving, the frequency-sensitive spillover framework developed here offers both immediate operational value and a durable foundation for adapting monetary policy to changing regional dynamics while preserving long-run price stability objectives. Most importantly, our findings demonstrate that effective inflation targeting in spatially heterogeneous economies requires moving beyond simple aggregate measures to understand the complex, frequency-dependent relationships that govern how price pressures propagate across regions and time horizons.

Data Availability

The CPI data used in this study are publicly available from Peru's National Institute of Statistics and Informatics (INEI). Replication code and processed datasets are available from the corresponding author upon reasonable request.

Funding

This research received no specific grant from any funding agency in the public, commercial, or not-for-profit sectors.

Conflicts of Interest

The authors declare no conflicts of interest

References

Alqaralleh, H. S., Canepa, A., and Muchova, E. (2025). Inflation synchronization and shock transmission between the eurozone and the non-euro cee economies: A wavelet quantile var approach. *The North American Journal of Economics and Finance*, 76:102334.

Antonakakis, N., Chatziantoniou, I., and Filis, G. (2014). Dynamic spillovers of oil price shocks and economic policy uncertainty. *Energy Economics*, 44:433–447.

Banco Central de Reserva del Perú (2023). Inflation report – december 2023. Technical report, Banco Central de Reserva del Perú.

Baruník, J. and Křehlík, T. (2018). Measuring the frequency dynamics of financial connectedness and systemic risk. *Journal of Financial Econometrics*, 16(2):271–296.

Batten, J. A., Ciner, C., and Lucey, B. M. (2015). Which precious metals spill over on which, when and why? some evidence. *Applied Economics Letters*, 22(6):466–473.

Bhoi, B. B., Shekhar, H., and Padhi, I. (2020). Rural-urban inflation dynamics in india. Technical report, Reserve Bank of India. Published in RBI Bulletin, December 2020.

Choi, J.-E. and Shin, D. W. (2020). Bootstrapping volatility spillover index. *Communications in Statistics-Simulation and Computation*, 49(1):66–78.

Colunga-Ramos, L. F. and Cepeda, L. T. (2023). Effects of supply, demand, and labor market shocks in the mexican manufacturing sector. Technical Report 2023-10, Banco de México.

de Guzmán, E. L. D. and Salas, E. (2023). La inflación en méxico 2021–2023. una explicación heurística. *ECONOMÍAUNAM*, 20(59):88–109.

Diebold, F. X. and Yilmaz, K. (2009). Measuring financial asset return and volatility spillovers, with application to global equity markets. *The Economic Journal*, 119(534):158–171.

Diebold, F. X. and Yilmaz, K. (2012). Better to give than to receive: Predictive directional measurement of volatility spillovers. *International Journal of forecasting*, 28(1):57–66.

Diebold, F. X. and Yilmaz, K. (2015). Measuring the dynamics of global business cycle connectedness. In Koopman, S. and Shephard, N., editors, *Unobserved Components and Time Series Econometrics*, pages 45–69. Oxford University Press, Oxford.

Elsayed, A. H., Hammoudeh, S., and Sousa, R. M. (2021). Inflation synchronization among the g7 and china: The important role of oil inflation. *Energy Economics*, 100:105332.

Fousekis, P. and Tzaferi, D. (2021). Returns and volume: Frequency connectedness in cryptocurrency markets. *Economic Modelling*, 95:13–20.

Gonzales de Olarte, E. (2003). Regiones integradas: Ley de incentivos para la integración y conformación de regiones lineamientos económicos y políticos. *Lima: Fondo Editorial del Congreso del Perú.*

Istiak, K., Tiwari, A. K., Husain, H., and Sohag, K. (2021). The spillover of inflation among the g7 countries. *Journal of Risk and Financial Management*, 14(8):392.

Jordan, T. J. (2016). The impact of international spillovers on swiss inflation and the exchange rate. *Journal of International Money and Finance*, 68:262–265.

Lucey, B. M., Larkin, C., and O'Connor, F. (2014). Gold markets around the world—who spills over what, to whom, when? *Applied Economics Letters*, 21(13):887–892.

Martins, M. M. F. and Verona, F. (2021). Inflation dynamics and forecast: Frequency matters. Research Discussion Paper 8/2021, Bank of Finland. Bank of Finland Research Discussion Papers.

Moreno, R. (2009). Some issues in measuring and tracking prices in emerging market economies. In *Participants in the meeting*, page 13.

Ndou, E. and Gumata, N. (2017). *Inflation Dynamics in South Africa: The Role of Thresholds, Exchange Rate Pass-through and Inflation Expectations on Policy Trade-offs*. Palgrave Macmillan.

Patton, A. (2013). Copula methods for forecasting multivariate time series. *Handbook of economic forecasting*, 2:899–960.

Pham, B. T. and Sala, H. (2022). Cross-country connectedness in inflation and unemployment: measurement and macroeconomic consequences. *Empirical economics*, 62(3):1123–1146.

Quineche, R., Aguilar, J., and Garibay, R. (2024). Analizando las expectativas de inflación de los agentes económicos durante el periodo pospandémico de covid-19 en latinoamérica. *Revista Moneda*, (198):4–9.

Tiwari, A. K., Shahbaz, M., Hasim, H. M., and Elheddad, M. M. (2019). Analysing the spillover of inflation in selected euro-area countries. *Journal of Quantitative Economics*, 17:551–577.

Wen, F., Zhang, K., and Gong, X. (2021). The effects of oil price shocks on inflation in the g7 countries. *The North American Journal of Economics and Finance*, 57:101391.

Winkelried, D. and Gutierrez, J. E. (2015). Regional inflation dynamics and inflation targeting. the case of peru. *Journal of applied economics*, 18(2):199–224.

Yglesias-González, M., Valdés-Velásquez, A., Hartinger, S. M., Takahashi, K., Salvatierra, G., Velarde, R., Contreras, A., Santa María, H., Romanello, M., Paz-Soldán, V., et al. (2023). Reflections on the impact and response to the peruvian 2017 coastal el niño event: Looking to the past to prepare for the future. *Plos one*, 18(9):e0290767.

Çakır, M. (2023). Regional inflation spillovers in turkey. *Economic Change and Restructuring*, 56(2):959–980.

Appendix A Supplementary Tables

Table A1: Sensitivity of time domain spillovers to the forecast horizon

Region	TO	FROM	NET
Lima	100.5 [88.03, 100.51]	76.51 [76.25, 76.51]	23.99 [11.78, 24]
Region 2	75.72 [75.71, 80.5]	75.99 [74.75, 75.99]	-0.27 [-0.27, 5.75]
Region 3	78.75 [78.74, 81]	78.26 [74.95, 78.27]	0.48 [0.48, 6.05]
Region 4	83.72 [83.72, 87.56]	78.51 [76.15, 78.51]	5.21 [5.21, 11.4]
Region 5	81.16 [74.94, 81.16]	76.19 [73.13, 76.19]	4.97 [1.81, 4.97]
Region 6	72.62 [61.29, 72.63]	68.44 [67.92, 68.44]	4.18 [-6.62, 4.19]
Region 7	84.65 [81.5, 84.65]	75.53 [74.59, 75.54]	9.11 [6.91, 9.12]
Region 8	39.74 [32.96, 39.75]	62.19 [54.13, 62.19]	-22.44 [-22.86, -21.18]
Region 9	46.33 [46.32, 48.8]	71.57 [64.71, 71.57]	-25.24 [-25.25, -15.91]
TSI		73.69 [70.73, 73.69]	

Note: This table shows the sensitivity of time domain spillovers to the forecast horizon (h = 1 to 12). Each cell reports the median value, with minimum and maximum across horizons in brackets. The lag of the VAR model is L=1, that was chosen by the BIC criterium.

Table A2: Sensitivity analysis of time domain spillovers with respect to VAR lag length

Region	**TO**	**FROM**	**NET**
Lima	96.67 [94.85, 100.43]	76.55 [75.82, 76.97]	20 [19.03, 23.94]
Region 2	76.6 [76.06, 78.03]	75.61 [74.62, 76.24]	1.19 [0.1, 2.99]
Region 3	79.72 [78.14, 80.54]	77.78 [76.65, 78.35]	2.01 [0.62, 3.18]
Region 4	85.56 [83.84, 87.12]	78.09 [76.72, 78.64]	7.85 [5.36, 9.47]
Region 5	80.93 [77.62, 82.34]	75.98 [75.08, 76.64]	4.81 [2.45, 5.7]
Region 6	71.63 [67.59, 72.13]	68.48 [67.18, 68.9]	2.8 [0.41, 3.76]
Region 7	84.5 [83.78, 84.69]	75.43 [74.83, 75.86]	8.83 [8.46, 9.87]
Region 8	39.98 [37.52, 41.55]	64.86 [61.93, 65.99]	-24.83 [-26.97, -22.62]
Region 9	47.53 [45.37, 49.18]	70.4 [68.78, 71.41]	-22.68 [-24.87, -21.2]
TSI		73.68 [72.89, 74.14]	

Note: Each cell reports the median value of the time domain spillover measure across different lag lengths, with the minimum and maximum in brackets. Spillovers are computed using a forecast horizon of $h = 3$, varying the lag length of the VAR model from $L = 1$ to $L = 6$.

Table A3: Time domain spillovers by cities

City	TO	FROM	NET
Abancay	71.8***	81.78***	-9.95
Arequipa	75.73***	79.17***	-3.44
Ayacucho	86.14***	82.63***	3.51
Cajamarca	56.93***	80.81***	-23.88***
Cerro de Pasco	100.32***	85.47***	14.85**
Chachapoyas	59.39***	83.13***	-23.75***
Chiclayo	102.58***	86.35***	16.22**
Chimbote	89.98***	85.17***	4.81
Cusco	72.52***	79.61***	-7.09
Huancavelica	78.48***	81.55***	-3.07
Huancayo	114.64***	83.15***	31.49***
Huánuco	82.07***	84.64***	-2.58
Huaraz	104.22***	85.70***	18.52**
Ica	87.45***	83.58***	3.87
Iquitos	33.65***	73.65***	-40.00***
Lima	**141.91*** **	**86.95*** **	**54.96*** **
Moquegua	99.35***	83.00***	16.36*
Moyobamba	56.45***	82.66***	-26.21***
Piura	95.17***	85.16***	10.01
Pucallpa	62.95***	77.61***	-14.66
Puerto Maldonado	27.92***	64.10***	-36.18***
Puno	60.87***	76.65***	-15.78*
Tacna	115.94***	81.57***	34.36***
Trujillo	94.55***	85.58***	8.97
Tumbes	70.88***	82.24***	-11.36
TSI		**73.68*** **	

Note: This table reports the time domain spillovers across cities of Peru. For the TSI, TO, FROM and NET spillover measures, we report statistical significance: *** significant at the 1% level, ** at the 5% level, and * at the 10% level.

Table A4: Frequency domain spillovers in the short, medium and long run

	Lima	Region 2	Region 3	Region 4	Region 5	Region 6	Region 7	Region 8	Region 9	FROM
Short run: Bands (π - $\frac{\pi}{3}$)										
Lima	11.85	5.74	6.41	6.69	5.53	2.99	6.50	1.07	3.11	38.04***
Region 2	5.34	12.59	7.02	7.22	3.84	3.02	4.80	1.09	3.11	35.43***
Region 3	4.82	5.57	10.48	5.21	3.05	2.03	4.26	0.95	2.64	28.55***
Region 4	5.80	6.33	5.80	11.57	4.31	2.70	5.16	1.24	2.70	34.06***
Region 5	5.17	3.73	3.61	4.54	10.88	2.53	4.39	1.38	3.13	28.47***
Region 6	3.64	3.88	3.03	3.61	3.26	12.45	3.25	4.05	2.17	26.89***
Region 7	5.01	4.18	4.43	4.87	3.99	2.43	10.10	1.57	2.77	29.25***
Region 8	1.70	1.63	1.35	1.85	1.96	4.93	2.67	15.66	1.78	17.87***
Region 9	3.31	3.40	3.41	3.09	3.28	1.62	3.12	1.14	13.37	22.38***
TO	34.81***	34.47***	35.06***	37.07***	29.22***	22.26***	34.14***	12.50***	21.42***	
NET	-3.24*	-0.96	6.51***	3.01	0.75	-4.62	4.89*	-5.37**	-0.96	**FSI = 28.99*** **
Medium run: Bands ($\frac{\pi}{3}$ - $\frac{\pi}{12}$)										
Lima	7.89	3.22	3.73	3.83	4.60	3.33	3.53	1.15	2.48	25.86***
Region 2	4.99	7.93	4.49	4.30	3.31	3.42	3.09	1.04	2.96	27.60***
Region 3	6.04	5.07	7.58	4.67	4.15	3.58	3.87	1.98	3.02	32.38***
Region 4	6.04	4.67	4.41	6.85	4.06	3.27	4.11	1.23	2.19	29.98***
Region 5	6.41	3.20	3.59	4.20	8.46	3.90	4.50	2.41	2.80	31.02***
Region 6	4.34	3.25	2.85	3.33	3.99	12.64	3.85	4.41	0.90	26.92***
Region 7	5.72	2.95	3.95	3.91	4.55	3.59	9.09	2.58	2.20	29.46***
Region 8	3.60	1.62	2.39	2.65	3.73	6.33	5.78	13.83	0.96	27.07***
Region 9	5.48	4.17	3.42	3.81	4.95	4.28	3.71	2.07	10.58	31.89***
TO	42.62***	28.16***	28.83***	30.69***	33.34***	31.70***	32.43***	16.87***	17.52***	
NET	16.76***	0.56	-3.55	0.72	2.32	4.79	2.97	-10.20***	-14.36***	**FSI = 29.13*** **
Long run: Bands ($\frac{\pi}{12}$ - 0)										
Lima	3.75	1.45	1.73	1.82	2.32	1.87	1.68	0.68	1.04	12.60***
Region 2	2.36	3.49	1.96	1.93	1.64	1.89	1.34	0.54	1.30	12.96***
Region 3	3.27	2.43	3.67	2.40	2.35	2.18	2.11	1.22	1.37	17.34***
Region 4	2.92	2.07	2.03	3.07	2.06	1.81	1.93	0.70	0.94	14.47***
Region 5	3.46	1.51	1.91	2.20	4.47	2.33	2.56	1.52	1.21	16.70***
Region 6	2.38	1.44	1.59	1.75	2.24	6.47	2.37	2.66	0.23	14.64***
Region 7	3.31	1.38	2.24	2.17	2.74	2.24	5.27	1.81	0.94	16.83***
Region 8	2.41	0.78	1.64	1.69	2.51	3.77	4.09	8.32	0.35	17.24***
Region 9	2.95	2.04	1.76	2.00	2.74	2.57	2.01	1.24	4.47	17.31***
TO	23.08***	13.09***	14.86***	15.96***	18.61***	18.65***	18.08***	10.38***	7.38***	
NET	10.48***	0.13	-2.47	1.49	1.91	4.01	1.25	-6.87**	-9.93***	**FSI = 15.57*** **

Note: This table reports the spillovers in the frequency domain. For the FSI, TO, FROM and NET spillovers measures, we report its statistical significance: *** significant at the 1% level, ** at the 5% level, and * at the 10% level.

Table A5: Frequency domain spillovers across cities: short run (π-$\frac{\pi}{3}$)

City	TO	FROM	NET
Abancay	27.49***	27.63***	-0.14
Arequipa	26.62***	30.07***	-3.45
Ayacucho	31.27***	34.04***	-2.76
Cajamarca	29.23***	31.73***	-2.50
Cerro de Pasco	42.86***	27.73***	15.14***
Chachapoyas	26.76***	23.69***	3.07
Chiclayo	44.27***	34.03***	10.24***
Chimbote	44.04***	41.22***	2.83
Cusco	24.51***	26.47***	-1.96
Huancavelica	33.19***	39.83***	-6.63
Huancayo	36.07***	32.77***	3.30
Huánuco	44.29***	36.15***	8.14**
Huaraz	45.34***	35.08***	10.26**
Ica	29.78***	30.74***	-0.96
Iquitos	17.82***	24.05***	-6.23
Lima	**51.12*** **	**43.97*** **	**3.14**
Moquegua	35.53***	35.16***	0.37
Moyobamba	27.61***	28.64***	-1.03
Piura	45.90***	42.10***	3.81
Pucallpa	21.87***	32.78***	-10.92***
Puerto Maldonado	9.59***	22.13***	-12.54***
Puno	18.90***	22.96***	-4.06
Tacna	31.60***	43.14***	-11.54***
Trujillo	42.91***	39.71***	3.21
Tumbes	35.72***	38.51***	-2.79
FSI		**32.97*** **	

Note: This table reports the spillovers in the frequency domain across cities in the short run (π-$\frac{\pi}{3}$). For the FSI, TO, FROM and NET spillovers measures, we report its statistical significance: *** significant at the 1% level, ** at the 5% level, and * at the 10% level.

Table A6: Frequency domain spillovers across cities: long run ($\frac{\pi}{3}$-0)

City	TO	FROM	NET
Abancay	44.88***	54.39***	-9.51
Arequipa	49.09***	49.19***	-0.10**
Ayacucho	55.52***	48.71***	6.80
Cajamarca	27.53***	49.19***	-21.65*
Cerro de Pasco	57.82***	57.92***	-0.09
Chachapoyas	32.71***	59.62***	-26.91**
Chiclayo	58.41***	52.38***	6.02**
Chimbote	45.77***	44.01***	1.76
Cusco	48.84***	53.36***	-4.51**
Huancavelica	45.59***	41.82***	3.78
Huancayo	79.44***	50.49***	28.95**
Huánuco	37.62***	48.62***	-11.01
Huaraz	59.39***	50.73***	8.65
Ica	58.19***	52.90***	5.29
Iquitos	15.69***	49.88***	-34.20***
Lima	**90.87*** **	**43.00*** **	**47.87*** **
Moquegua	63.68***	47.91***	15.76
Moyobamba	28.64***	54.14***	-25.50***
Piura	48.54***	43.08***	5.46
Pucallpa	40.97***	44.97***	-4.00
Puerto Maldonado	18.66***	42.59***	-23.93**
Puno	42.71***	54.25***	-11.54
Tacna	84.87***	38.52***	46.35***
Trujillo	51.23***	45.92***	5.31
Tumbes	34.74***	43.79***	-9.05
FSI		**48.86*** **	

Note: This table reports the spillovers in the frequency domain across cities in the long run ($\frac{\pi}{3}$-0). For the FSI, TO, FROM and NET spillovers measures, we report its statistical significance: *** significant at the 1% level, ** at the 5% level, and * at the 10% level.

Appendix B Supplementary Figures

Figure B1: Dynamic FROM spillovers to all others in the short run

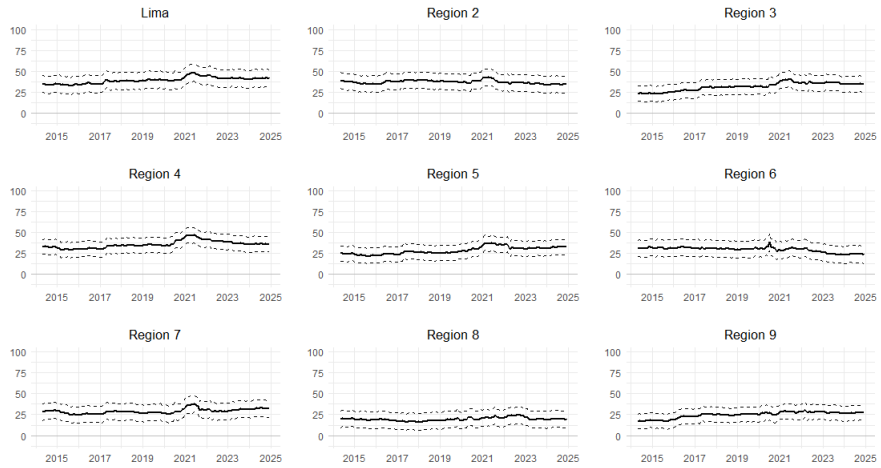

Note: This figure shows the short-term FROM spillovers (π, $\frac{\pi}{3}$), estimated using the BK methodology (Baruník and Křehlík, 2018). Results are based on a rolling window of 150 observations. Dashed lines indicate 95% confidence intervals from 5,000 pivot bootstrap simulations (Choi and Shin, 2020).

Figure B2: Dynamic FROM spillovers to all others in the long run

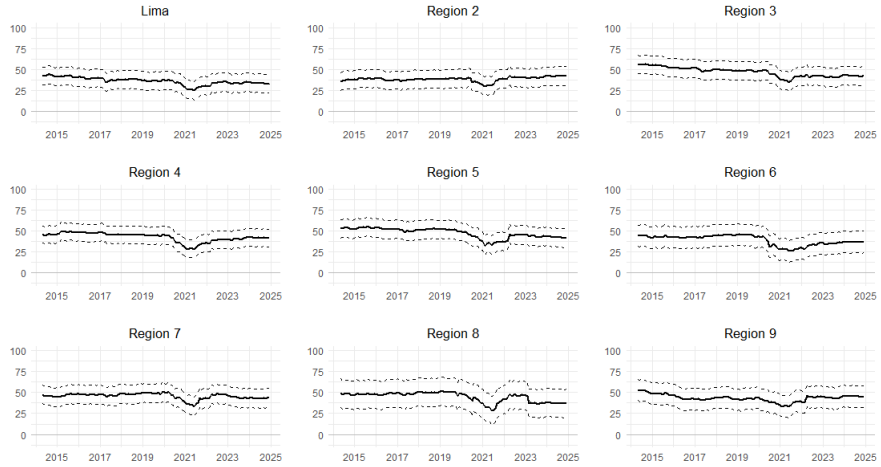

Note: This figure shows the long-term FROM spillovers ($\frac{\pi}{3}$, 0), estimated using the BK methodology (Baruník and Křehlík, 2018). Results are based on a rolling window of 150 observations. Dashed lines indicate 95% confidence intervals from 5,000 pivot bootstrap simulations (Choi and Shin, 2020).

Figure B3: Robustness of Dynamic NET Spillovers to Forecast Horizon

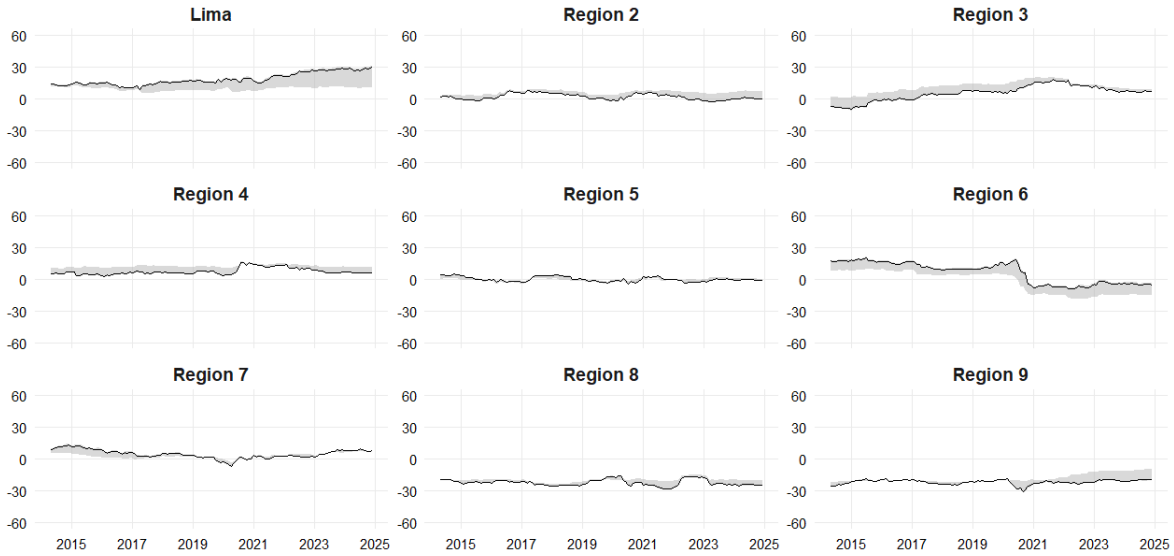

Note: This figure shows the evolution of net inflation spillovers across regions using the Diebold and Yilmaz (2012) methodology. Estimates are based on a fixed lag length 1 and a rolling window of 150 observations, while the forecast horizon H varies from 1 to 12. The solid black line represents the median net spillover across horizons, and the shaded area reflects the range between the minimum and maximum values.

Figure B4: Robustness of Dynamic NET Spillovers to Lag Length

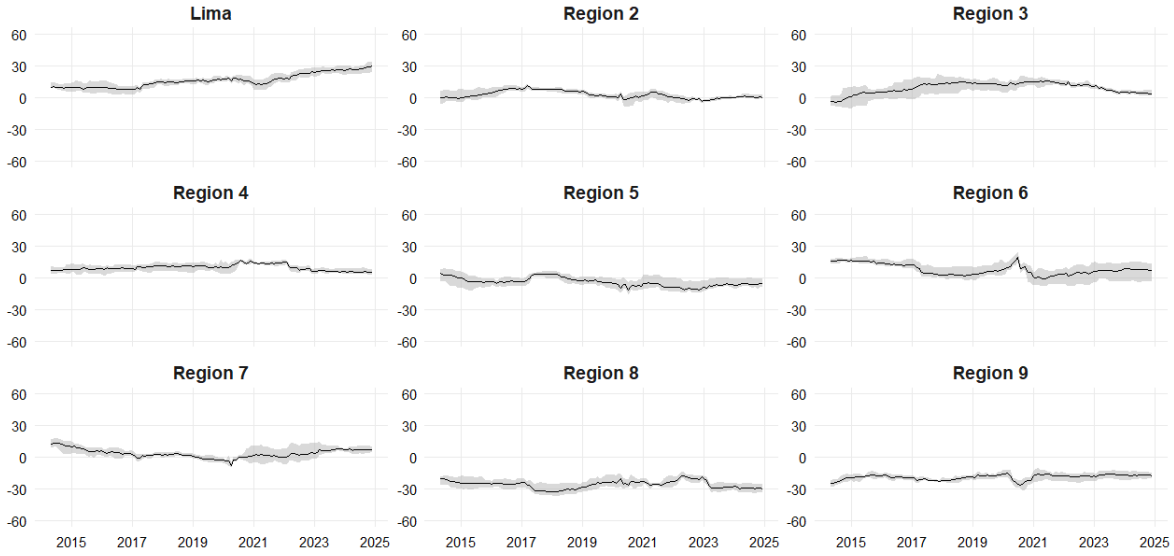

Note: This figure displays the evolution of net inflation spillovers across regions using the Diebold and Yilmaz (2012) methodology. Estimates are based on a fixed forecast horizon $H = 3$ and a rolling window of 150 observations, while the lag length varies from 1 to 6 to assess the robustness of results to alternative lag specifications.

Figure B5: Robustness of Dynamic NET Spillovers to Rolling Window Size

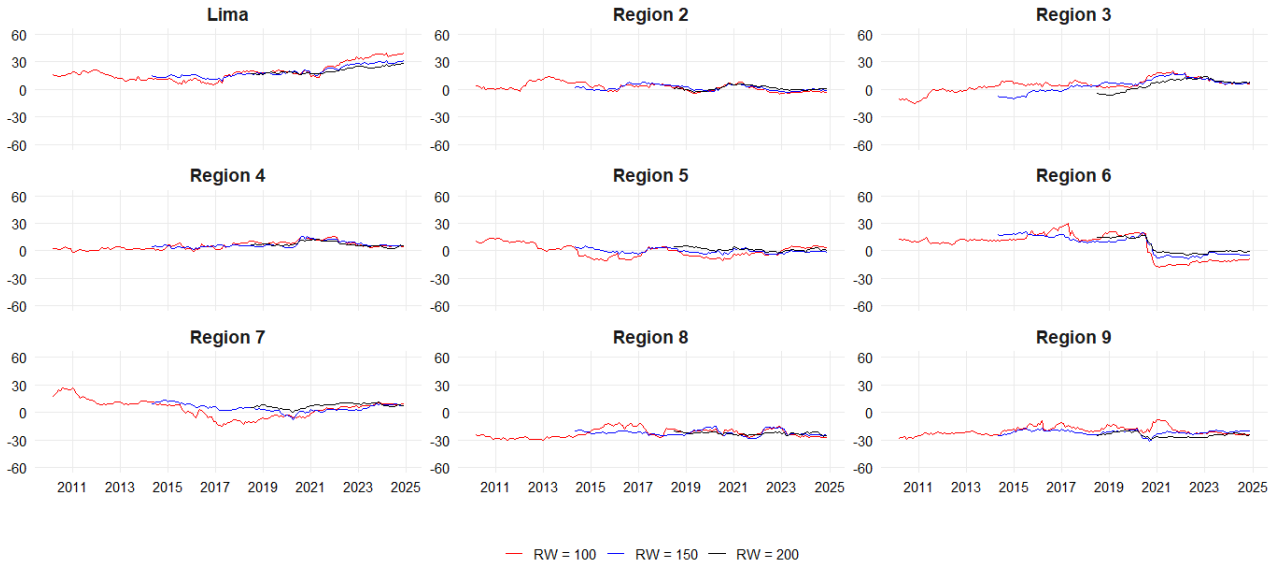

Note: This figure displays the evolution of net inflation spillovers across regions using the Diebold and Yilmaz (2012) methodology. Estimates are based on a fixed forecast horizon of 3 and a lag length of 1, while the rolling window size varies across 100, 150, and 200 observations.

Figure B6: Dynamic NET spillovers in the short, medium and long run

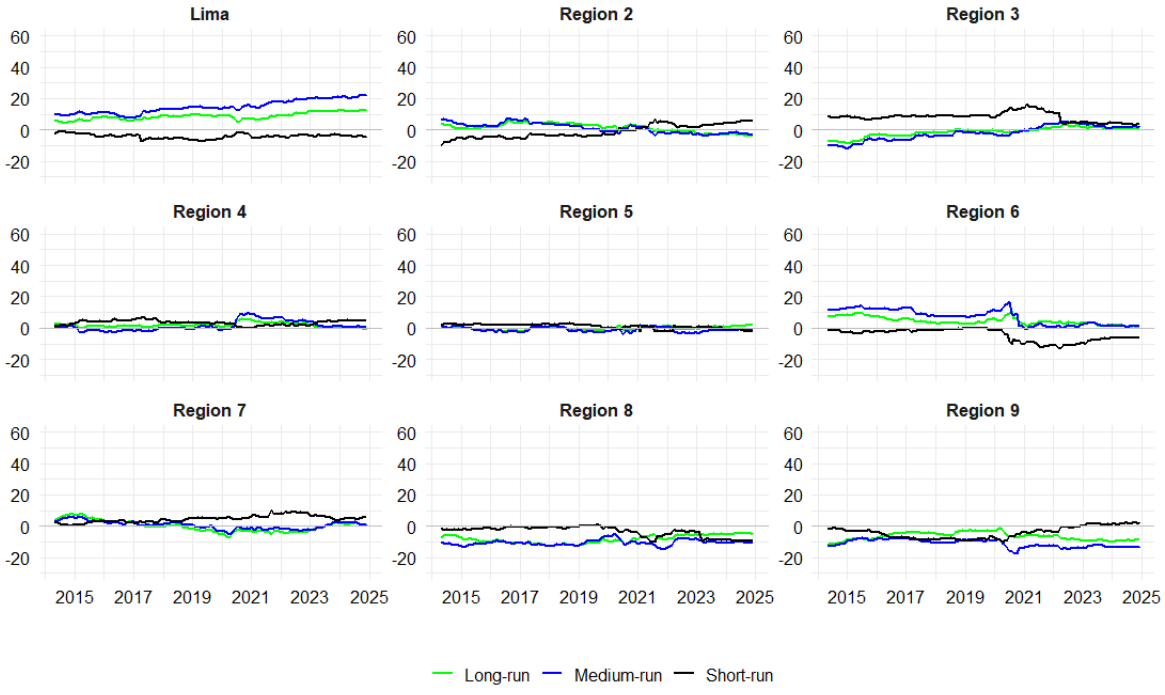

Note: This figure shows the short-term NET spillovers (π, $\frac{\pi}{3}$), medium-term NET spillovers ($\frac{\pi}{3}$, $\frac{\pi}{12}$) and long-term NET spillovers ($\frac{\pi}{12}$, 0), estimated using the BK methodology (Baruník and Křehlík, 2018). Results are based on a rolling window of 150 observations.